AD-A210 341

June 1989
POLY-WRI-1560-89

FINAL TECHNICAL REPORT
on
PHYSICS OF HIGH ENERGY
PHOTOCONDUCTIVE SWITCHES
August 1, 1985 - September 30, 1988

E. E. Kunhardt
Weber Research Institute
Polytechnic University
Route 110, Farmingdale, New York 11735

Prepared for

Department of the Air Force
Air Force Office of Scientific Research

under

Grant No. AFOSR-85-0249

89 7 19 028

REPORT DOCUMENTATION PAGE

1a. REPORT SECURITY CLASSIFICATION Unclassified		1b. RESTRICTIVE MARKINGS			
2a. SECURITY CLASSIFICATION AUTHORITY		3. DISTRIBUTION/AVAILABILITY OF REPORT			
2b. DECLASSIFICATION / DOWNGRADING SCHEDULE		Approved for public release; distribution unlimited.			
4. PERFORMING ORGANIZATION REPORT NUMBER(S)		5. MONITORING ORGANIZATION REPORT NUMBER(S) AFOSR-TR- 89-0994			
6a. NAME OF PERFORMING ORGANIZATION Polytechnic University Weber Research Institute	6b. OFFICE SYMBOL (If applicable)	7a. NAME OF MONITORING ORGANIZATION Air Force Office of Scientific Research			
6c. ADDRESS (City, State, and ZIP Code) Route 110 Farmingdale, NY 11735		7b. ADDRESS (City, State, and ZIP Code) BKG 410 Bolling Air Force Base, D. C. 20332-6448			
8a. NAME OF FUNDING/SPONSORING ORGANIZATION Air Force Office of Scientific Research	8b. OFFICE SYMBOL (If applicable) NP	9. PROCUREMENT INSTRUMENT IDENTIFICATION NUMBER AFOSR-85-0249			
8c. ADDRESS (City, State, and ZIP Code) BKG 410 Bolling Air Force Base, DC 20332-6448		10. SOURCE OF FUNDING NUMBERS			
		PROGRAM ELEMENT NO. 61102F	PROJECT NO. 2301	TASK NO. A7	WORK UNIT ACCESSION NO.

11. TITLE (Include Security Classification)
"Physics of High Energy Photoconductive Switches"

12. PERSONAL AUTHOR(S)
Erich E. Kunhardt

13a. TYPE OF REPORT Final Technical	13b. TIME COVERED FROM 8/1/85 TO 9/30/88	14. DATE OF REPORT (Year, Month, Day) June 1989	15. PAGE COUNT 25

16. SUPPLEMENTARY NOTATION

17.	COSATI CODES		18. SUBJECT TERMS (Continue on reverse if necessary and identify by block number)
FIELD	GROUP	SUB-GROUP	Macro-kinetic Electron Energy distribution
	20 09		Semiconductor Transport Parameters Rate coefficients

19. ABSTRACT (Continue on reverse if necessary and identify by block number)

During this funding period, a semi-classical macro-kinetic theory that describes the dynamic behavior of carriers in a semiconductor under the influence of space-time varying fields has been formulated. The macro-kinetic model is considerably easier to implement numerically than Monte Carlo methods or those based on the Boltzmann Transport Equation (BTE). Moreover, the macro-kinetic model requires orders of magnitude less computer time to run. A Monte Carlo method has been developed for obtaining the electron energy distribution, transport parameters, and rate coefficients in multi-valley semiconductors. The procedure requires an order of magnitude less time than conventional Monte Carlo techniques.

20. DISTRIBUTION/AVAILABILITY OF ABSTRACT ☒ UNCLASSIFIED/UNLIMITED ☐ SAME AS RPT ☐ DTIC USERS	21. ABSTRACT SECURITY CLASSIFICATION Unclassified	
22a. NAME OF RESPONSIBLE INDIVIDUAL Bruce L. Smith, Lt Col, USAF	22b. TELEPHONE (Include Area Code) 202-767-4908	22c. OFFICE SYMBOL NP

DD FORM 1473, 84 MAR

83 APR edition may be used until exhausted.
All other editions are obsolete.

ABSTRACT

During this funding period, a semi-classical macro-kinetic theory that describes the dynamic behavior of carriers in a semiconductor under the influence of space-time varying fields has been formulated. The macro-kinetic model is considerably easier to implement numerically than Monte Carlo methods or those based on the Boltzmann Transport Equation (BTE). Moreover, the macro-kinetic model requires orders of magnitude less computer time to run. A Monte Carlo method has been developed for obtaining the electron energy distribution, transport parameters, and rate coefficients in multi-valley semiconductors. The procedure requires an order of magnitude less time than conventional Monte Carlo techniques.

/

\ \

I. OVERVIEW OF RESEARCH PROGRAM

I. INTRODUCTION

High Power Semiconductor Switches (HPSS) are receiving considerable attention for the promise they offer to pulse power technology.[1-3] This promise is founded on the fact that with semiconducting materials as the switching medium, it is possible to obtain: (a) high current densities over large areas, (b) high carrier production and relaxation rates, (c) conductivity modulation over several orders of magnitude, and (d) high dielectric field strengths. HPSS may be developed that have lower inductance and forward drop, higher rep-rate, longer lifetime, and are more compact than comparable gas switches. In addition, simple and compact (re-usable) opening switches and other pulse power devices (such as frozen wave generators) seem to be realizable with semiconductor switching technology.[3] Optically or electrically triggered bulk and junction devices and externally controlled bulk devices are being investigated in a variety of geometries and covering a wide range of parameters.[1-3] Semiconducting materials that have been considered are Si, III-V's, and diamond.

With AFOSR support, our research activities have focused on the basic physics of HPSS devices. Our aim has been to develop a quantitative understanding of the role of the various microscopic processes, material parameters, trap dynamics, and space-charge in shaping the behavior of HPSS. This knowledge is necessary for guiding the scaling of the present low power technology to the regime of interest in pulse power applications. Moreover, with sufficient understanding, it may be possible to tailor the electrical properties of semiconductor materials (beyond that of density modulation) for specific applications. During this contract period, we have developed models for describing the dynamics of the carriers under the influence of space-time varying fields. In the next section, a summary of the accomplishments made during the period of this contract is given. Sections III and IV are devoted to a detailed discussion of the results obtained.

II. REVIEW OF ACHIEVEMENTS AND ACTIVITIES DURING THE CONTRACT PERIOD

During this past funding period we have accomplished the following:

(1) A semi-classical macro-kinetic theory that describes the dynamic behavior of carriers in a semiconductor under the influence of space-time varying fields has been formulated. It is essentially a "properly closed" set of moment equations. That is, a macro-kinetic distribution is introduced and the equation of evolution for this distribution is used to close the moment equations. In this fashion, the transport parameters and rates that appear in the moment equations can be determined from first principles (in particular, without phenomenological assumptions regarding the form of distribution). This is particularly important for describing high field transport in "multi-valley" semiconductor materials such as gallium arsenide (GaAs) (see next section).

A single valley macro-kinetic model has been developed and compared to exact Monte Carlo simulations of carrier dynamics in GaAs and the results have been found to be in reasonably good agreement. The macro-kinetic model is considerably easier to implement numerically than Monte Carlo methods or those based on the Boltzmann Transport Equation (BTE). Moreover, the macro-kinetic model requires orders of magnitude less computer time to run. This theory has been published in a paper that appeared in the Journal of Applied Physics (August 1988) and is presented in Section III. This theory is now being used to develop a three valley moment model of carrier transport in multi-valley semiconductors.

A Monte Carlo method has been developed for obtaining the electron energy distribution, transport parameters, and rate coefficients in multi-valley semiconductors. The procedure requires an order of magnitude less time than conventional Monte Carlo techniques. The technique has been discussed in a paper that appeared in the Journal of Applied Physics (April 1988) and is presented in Section IV. At present, a number of papers relating other results that have been obtained are in preparation.

Published Papers:

1. "Nonequilibrium Macroscopic Models of Carrier Dynamics in a Semiconductor," J. Appl. Phys. 64, 1220 (1988) (with M. Cheng and C. Wu).

2. "Electron Energy Distributions, Transport Parameters, and Rate Coefficients in GaAs," J. Appl. Phys. 63, 2322 (1988) (with M. Cheng).

A number of presentations were also made during this period at various workshops on HPSS sponsored by both ONR and AFOSR. Abstracts for papers presented at the spring meeting of the American Physical Society are given in Section V. Also during this period, one student (M. Cheng) received his MS degree and is currently working on his Ph.D. We were invited to visit a number of government laboratories that have shown interest in our results (Harry Diamond and EDTL/Fort Monmouth Laboratories).

1. M. Kristiansen and W. Portnoy, Workshop on Solid State Switches for Pulsed Power, Tamaron, Colorado, January 1983.

2. B. Senitzky, Workshop on New Direction in Solid State Power Switches, Polytechnic University, Farmingdale, NY, 1985.

3. K. H. Schoenbach and M. Weiner, Workshop on Optically and Electron-Beam Controlled Semiconductor Switches, Norfolk, VA, 1988.

III. NONEQUILIBRIUM MACROSCOPIC MODELS OF CARRIER DYNAMICS IN A SEMICONDUCTOR

I. INTRODUCTION

The dynamic behavior of free carriers in a semiconductor under the influence of a field may be described in the semi-classical regime by the time-dependent distribution function $f(\kappa, r, t)$ (where κ is the carrier momentum, r is its position, and t is time).[1,2] Given the initial state of the carriers, the distribution function at any other time may be obtained from either the Boltzmann transport equation (BTE),[2-5] or from Monte Carlo simulations.[6,7] When the fields are changing in space time it is, in general, very difficult to obtain the solution to the BTE. Moreover, the Monte Carlo approach, although simple to implement, is very time consuming and in some cases (depending on the number of test particles used) prohibitive. Once the distribution function is found, desired macroscopic properties (which can be measured) can be calculated by averaging the corresponding microscopic properties over the distribution.[1,8]

An alternate approach for obtaining the macroscopic state of the carriers is in terms of moments of the distribution. In general, an exact description of the state requires an infinite set of moments (this is equivalent to the fact that we need an infinite set of moments to specify the distribution f). These moments obey a hierarchy (infinite set) of equations obtained by taking moments of the BTE.[9] It will be assumed that for the situations of interest a finite set of moment equations can be used to describe the behavior of the carriers.[9] To assess the accuracy of this finite set, the results for some representative cases must be compared with those obtained from the exact distribution function.

This paper focuses on how to obtain a closed set of moment equations which are valid in the presence of space-time varying fields. This subject has recently received considerable attention because of the deficiency of the drift-diffusion equation in the analysis of high-frequency and submicron devices.[10-13] The drift-diffusion equation is based on the assumption that the carrier momentum distribution is in equilibrium with the local, instantaneous, applied field. This restricts the validity of the equation to slowly varying fields and large-size devices.[13] However, for (semiclassical) devices with very small spatial and/or temporal scales, nonequilibrium phenomena, such as velocity overshoot,[11,14] dominate the transport behavior of carriers. In this case, the use of BTE or an equivalent nonequilibrium set of moment equations is essential.

A number of approaches have been proposed for obtaining a closed set of moment equations. These approaches can be divided into three general categories, each based on the respective assumption that (a) for small electric fields the distribution function can be represented by two terms in an expansion in terms of Legendre polynomials,[15,16] (b) the distribution function is a displaced Maxwellian[17-19] when the carrier concentration is sufficiently high, and (c) the unknown variables and coefficients appearing in the moment equations are assumed to be functions of mean energy only and are obtained from phenomenological equations.[20,21] The first approach is closest in spirit to a derivation based on first principles. This is important since it can provide guidance as to where the model is likely to fail.

In the next section, a mathematical formulation of the problem and the foundation for an approach to its solution is presented. This approach is based on the fact that the moment equations vary in a slower space/time scale than the BTE. Since little is known about the properties of the scattering operators in the BTE for the case of a semiconductor, we have used the physical knowledge derived from the moment equations to implement an averaging scheme over the fast variations of the BTE. It is shown that it is sufficient to use the characteristic times of the moment equations to effect a truncation scheme and prescribe a procedure for arriving at a closed set of equations. This approach has also been discussed in connection with electron dynamics in gases.[22] In Sec. III, closed sets of moment equations are derived for three levels of description. These equations have been used to describe the behavior of electrons in GaAs subjected to step fields. Although, the method presented in this paper can be used to derive a multivalley macroscopic model, a single-valley model has been used for GaAs. The results for the average velocity and mean energy obtained with this formulation are compared with those obtained using Monte Carlo methods. For the Monte Carlo calculations, a three-valley model for GaAs has been used. The results from these two models are in reasonably good agreement. However, the single-valley model in this case does not provide an accurate description of the behavior at electric fields above the threshold field (about 3.5 kV/cm for GaAs) for the Gunn effect due to strong intervalley scatterings. Some concluding remarks are given in Sec. V.

II. FORMULATION OF THE NONEQUILIBRIUM MACROSCOPIC DESCRIPTION

For simplicity in notation (so that subscripts referring to different types of carriers need not be introduced), the discussion will focus on the dynamics of electrons in a single valley. A similar treatment holds for electrons in other valleys (also for holes in the valence band), with proper considerations given to interactions between the various valleys and types of carriers. Extension to multivalley description is straightforward. The situations of interest may be described by a distribution function in (κ, r) space, $f(\kappa, r, t)$. This function obeys the BTE; namely,[1,2]

$$\partial_t f + v \cdot \nabla_r f + (q/\hbar) E \cdot \nabla_\kappa f = I(f), \qquad (1)$$

where v is the macroscopic carrier velocity, $E = E(r, t)$ is the electric field (either externally applied or arising from space charge), and $I(f)$ is the linear scattering operator. v is defined as the κ-space gradient of the microscopic energy ϵ; that is, $v = \hbar^{-1} \nabla_\kappa \epsilon(\kappa)$. No specific form for the operator I need be assumed at this time. This operator describes a number of physical processes (interactions between carriers and lattice) which occur in different space-time scales. The scales of interest are the fine-grained (kinetic), where

changes occur in a particular scattering time distance, and the coarse-grained hydrodynamics, where changes occur in a macroscopic scale.

At the macroscopic level, the state of the carriers in a semiconductor is given by the state vector (of finite dimension) S, whose components are moments of the distribution. That is, $S_N = [m(r,t), j = 1, N]$, where m corresponds to a moment of the distribution which may be a scalar, vector, or tensor,[1] and N corresponds to the highest moment kept in the description. The equations for the moments are obtained by taking appropriately weighted integrals (in κ space) of Eq. (1).[1,2] The equations for the first three moments [namely, density $n(r,t)$, mean energy $\bar{\epsilon}(r,t)$, and average momentum $\kappa(r,t)$], are

$$\partial_t n + \nabla \cdot (n\mathbf{u}) = vn, \tag{2a}$$

$$\partial_t (n\bar{\epsilon}) + \nabla \cdot \langle \epsilon v \rangle - q\mathbf{E} \cdot n\mathbf{u} = -v_\epsilon n\bar{\epsilon}, \tag{2b}$$

$$\partial_t (n\bar{\kappa}) + \nabla \cdot \langle \kappa v \rangle - q\mathbf{E}/n = -v_m n\bar{\kappa}, \tag{2c}$$

where the bracket implies an average over the distribution, $\mathbf{u}$ is the average velocity $[= \int vf\,d\kappa = \hbar^{-1} \int \nabla_\kappa \epsilon(\kappa) f\,d\kappa]$, and v, v_ϵ, and v_m are the (space-time dependent) effective-carrier-gain, energy exchange, and momentum exchange frequencies. These frequencies are defined by

$$vn = \int I(f)\,d\kappa, \tag{3a}$$

$$v_\epsilon n\bar{\epsilon} = \int \epsilon(\kappa) I(f)\,d\kappa, \tag{3b}$$

$$-v_m n\bar{\kappa} = \int \kappa I(f)\,d\kappa. \tag{3c}$$

Since it is difficult to ascribe physical significance to higher-order moments, their equations of evolution are seldom written.

Unfortunately, any finite set of moment equations is not determinate.[8] For example, the set of Eqs. (2) contains unknown averages over the distributions (quantities in brackets) and unknown rates [Eqs. (3)]. To calculate these unknowns and thus arrive at a determinate set of equations for S_N, f needs to be found. A similar problem arises in classical gas kinetics,[23,24] and in electron kinetics in ionized gases.[22] In contrast to classical gas dynamics and in similarity with ionized gases, very little is known about the properties of either $I(f)$, or the operator $(q/\hbar)\mathbf{E} \cdot \nabla_\kappa - I(f)$ in Eq. (1). Because of this, a more physical approach is proposed for closing the moment equations. The key to this approach is the use of information from the macroscopic equations to effect the truncation. This is outlined below.

First, the moment equations are ordered according to their characteristic scales. This step requires *a priori* assumptions about the relative magnitude of these scales. They can be made from physical considerations. In any event, the ordering that is used needs to be confirmed after the solution has been found. Equations (2a)–(2c) have been ordered according to their characteristic times. These times are (in decreasing magnitude): τ (effective carrier production/loss time), τ_ϵ (energy exchange time), and τ_m (momentum exchange time). The higher moment equations would also have to be ordered accordingly. It is assumed that their char-

acteristic times are smaller than those defined above. Note that, in general, $\tau_\epsilon > \tau_m$ in a semiconductor.[13]

Next, the number of moments in the state vector S_N is determined from physical consideration, and from the scale of the desired description. Alternatively, the number of moments that are used determines the coarseness of the macroscopic description. This is because the model is only valid for time scales of the order of the smallest characteristic time contained in a finite set of equations.

Finally, note that the distribution function f which satisfies Eq. (1) contains information to all orders of time greater than a microscopic scattering time.[1,2,25] The microscopic scattering time is, in general, much smaller than the characteristic times in any finite set of moment equations. The distribution function f contains "too much information" compared to the state vector S_N in the scale of the desired description. That is, the unknown variables and parameters in the S_N description do not follow the fast variations in f. Thus, to obtain a determinate set of moment equations, it is sufficient to use an "f" which only contains information in the scale of the moment equations. This distribution, the macroscopic distribution function f_M, obeys a "macroscopic-kinetic equation." The equation of evolution for f_M, together with the finite set of moment equations, form a closed set. This set can be used to describe the nonequilibrium dynamics of the carriers in a time scale corresponding to the characteristic times of the moment equations. This description is termed nonequilibrium because f_M may be space-time dependent. In fact, in the time scale of the moments, it is equivalent to f.

A number of procedures can be used to arrive at an equation for f_M. The objective in any of these procedures is to change the scale of Eq. (1) from the microscopic to that of the finite set of moment equations.[26,27] In this paper, the technique proposed by Bogoliubov is used.[26] A problem arises when trying to solve the equation for f_M. This has to do with the issue of assignment of initial values to f_M.[23] In this paper, it will be assumed that the moments of f_M correspond to the (approximate) macroscopic state. To solve the equations for f_M, it is still necessary to know the various microscopic scattering processes for electrons in a given semiconductor. After solving for f_M, Eqs. (2) and (3) can be used to describe the electron dynamics in the semiconductor (see Sec. IV). The procedure outlined above is used in the next section to obtain closed sets of moment equations valid in three different regimes (time scales).

III. THE NONEQUILIBRIUM MACROSCOPIC EQUATIONS

The approach outlined in the previous section will now be used to obtain the nonequilibrium macroscopic equations. The characteristic times of the macroscopic equations [Eqs. (2a)–(2c)] can be used to define various levels of descriptions. The most coarse-grained description is valid for times in the order of τ (see Sec. II). From Eqs. (2a)–(2c), since $v < v_\epsilon < v_m$, there is a time for which the mean energy and average momentum of the carriers have relaxed to a state of quasiequilibrium where their subsequent vari-

ation is in the scale of τ, i.e., the scale of the density varia-
tions. For such times, the macroscopic evolution of the sys-
tem can be described in a single time scale τ. Thus,
$S_1 = [n(r,t)]$; that is, the macroscopic state vector contains
a single moment, the density.

Progressively less coarse-grained levels of description
can be defined by systematically using an additional moment
in the state vector. This assumes that the characteristic times
in the moment equations are not degenerate (i.e., character-
istic times are not equal). In this case, these are times for
which the higher-order moments have relaxed to a state in
which their scale of variation is the same as the moments
being used in the characterization of the macroscopic state.
If there was a degeneracy (for example, $v_\epsilon^{-1} = v_m^{-1}$), then
the corresponding moments must be collectively taken as
components of the state vector. For cases of interest (carri-
ers in a semiconductor), the characteristic times are not, in
general, degenerate.[8] Thus, the next less coarse-grained level
of description is in terms of $S_2 = [n(r,t),\bar{\epsilon}(r,t)]$. This is val-
id for times in the order of v_ϵ^{-1}. From a practical point of
view, the least coarse-grained description of interest is in
terms of $S_3 = [n(r,t),\bar{\epsilon}(r,t),\bar{\kappa}(r,t)]$, which is valid for times
of the order of v_m^{-1}.

To make the equations that define the macroscopic
state, S_i, $i = 1,2,3$, determinate, the macroscopic-kinetic
distribution, f_M, must be found. The time scale of f_M must be
consistent with the level of description. Thus, a macroscopic
equation of evolution for f_M needs to be derived and solved.
This is carried out below for each level of description of in-
terest; namely, S_i, $i = 1,2,3$.

A. The S_1 state (defined for times $\sim v^{-1}$)

In this case, only Eq. (2a) and the equation for
$f_M = f_M^1$ in the τ time scale are necessary to describe the
evolution of the carriers. These two equations form a closed
set. The equation for f_M is obtained by changing the time
scale of the BTE [Eqs. (1)] from the fine-grained to a τ
scale. This can be achieved using a technique introduced by
Bogoliubov.[20] Mathematically, the change can be accom-
plished by the following relation:

$$f(\kappa,r,t) = f_M^1[\kappa,n(r,t)].\tag{4}$$

That is, in the τ scale, the space-time dependence of the dis-
tribution is not explicit, but implicit through a dependence
on the density. The equation governing the changes in f_M^1
can be found using Eqs. (1) and (2a). From Eq. (4), the
changes in f can be written as

$$\partial_t f = \partial_n f_M^1 \partial_t n,\tag{5a}$$

$$\nabla_r f = \partial_n f_M^1 \nabla_r n,\tag{5b}$$

$$\nabla_\kappa f = \nabla_\kappa f_M^1.\tag{5c}$$

Subsequently, the subscript r is to be dropped from the space
gradient. The time derivative of the density may be eliminat-
ed from Eq. (5a) by using Eq. (2a), rewritten in the form

$$\partial_t n = -\int \partial_n f_M^1 v \, d\kappa \cdot \nabla n + \int I(f_M^1) d\kappa.\tag{6}$$

After placing Eqs. (5) and (6) into Eq. (1), the following
equation is obtained for the distribution:

$$\partial_n f_M^1 \left(-\int \partial_n f_M^1 v \, d\kappa \cdot \nabla n + \int I(f_M^1) d\kappa \right)$$
$$+ v \cdot \nabla n \partial_n f_M^1 + (qE/\hbar) \cdot \nabla_\kappa f_M^1 = I(f_M^1).\tag{7}$$

If the deviation from spatial uniformity is small, a parameter
δ can be introduced into Eq. (7) which is indicative of this
assumption. Using δ as a basis for a perturbation expansion,
the distribution may be expressed as

$$f_M^1(\kappa,n) = \sum_i \delta^i f_{M_i}^1(\kappa,n).$$

which substituted into Eq. (7) results in the following equa-
tions:

$$\sum_{i,j} \delta^{i+j+1} \partial_n f_{M_i}^1 \left(-\int \partial_n f_{M_j} v \, d\kappa \cdot \nabla' n \right)$$

$$+ \sum_{i,j} \delta^{i+j} \partial_n f_{M_i}^1 \int I(f_{M_j}^1) d\kappa$$

$$+ \sum_i \delta^{i+1} (\partial_n f_{M_i}^1 v \cdot \nabla' n)$$

$$+ \sum_i \delta^i \frac{q}{\hbar} E \cdot \nabla_\kappa f_{M_i}^1 = \sum_i \delta^i I(f_{M_i}^1),\tag{8}$$

where $r \to \delta^{-1} r'$; $\nabla \to \delta \nabla'$. From Eq. (8), the zeroth order
equation is found to be

$$(q/\hbar)E \cdot \nabla_\kappa f_{M_0}^1(\kappa,n) = I(f_{M_0}^1) - \partial_n f_{M_0}^1 \int I(f_{M_0}^1) d\kappa,$$

which has the general solution

$$f_{M_0}^1(\kappa,n) = f_{M_0}^1(\kappa)n(r',t),\tag{9}$$

where $f_{M_0}^1(\kappa)$ obeys the equation

$$(q/\hbar)E \cdot \nabla_\kappa f_{M_0}^1(\kappa) = I(f_{M_0}^1) - f_{M_0}^1(\kappa) \int I(f_{M_0}^1) d\kappa.\tag{10}$$

with the condition

$$\int f_{M_0}^1(\kappa) d\kappa = 1.\tag{11}$$

Note that the same symbol has been used for $f_{M_0}^1(\kappa,n)$ and
$f_{M_0}^1(\kappa)$. The context in which they are used determines the
argument. Equation (10) has the form of a steady state, ho-
mogeneous Boltzmann equation, and $f_{M_0}^1$ can be identified
as the (zeroth order) steady-state distribution of a homo-
geneous assembly of carriers in a field defined by the local
value of the field. This is the distribution that exists at (r',t)
if local equilibrium with the field is assumed. A number of
techniques are available for solving this equation.[3] $f_{M_0}^1$ can
also be obtained using Monte Carlo methods.[6] Noting from
Eq. (9) that $\partial_n f_{M_0}^1(\kappa,n) = f_{M_0}^1(\kappa)$, the equation of $O(\delta)$ is
found from Eq. (8) to be

$$qE \cdot \nabla_\kappa f_{M_1}^1 - I(f_{M_1}^1) + f_{M_0}^1 \int I(f_{M_1}^1) d\kappa$$

$$= f_{M_0}^1 \int f_{M_0}^1 v \, d\kappa \cdot \nabla' n$$

$$- f_{M_0}^1 v \cdot \nabla' n - n f_{M_0}^1 \int I(f_{M_0}^1) d\kappa,\tag{12}$$

where the last term is an approximation to the correspond-

ing term in Eq. (8)

Linearizing Eq. (12), and treating the right-hand side as
a source, the solution to Eq. (12) may be formally written as

$$f^1_M(\kappa,r) = \int G(\kappa,\kappa') S(\kappa',r) d\kappa'.$$ (13)

where S is the RHS of Eq. (12), and G is the Green's func-
tion of a linearized Eq. (10). Substituting for S in Eq. (13),

$$f^1_M(\kappa,r) = f^1_{M_a} n + f^1_{M_b} \cdot \nabla n.$$ (14a)

where

$$f^1_{M_b} = \int G(\kappa,\kappa') \left(f^1_M(\kappa') \int f^1_M(\kappa'') \right.$$
$$\left. \cdot v(\kappa'') d\kappa'' - f^1_M(\kappa') v(\kappa') \right) d\kappa'.$$ (14b)

and

$$f^1_{M_a} = - \int G(\kappa,\kappa') f^1_M(\kappa')$$
$$\cdot \left(\int I [f^1_M(\kappa'')] d\kappa'' \right) d\kappa'.$$

Since $\int f^1_M d\kappa = 0$ (note that $\int f d\kappa = n$ and $\int f^1_M d\kappa$ has
been taken to be one), the f^1_M's above must satisfy the
conditions $\int f_{M_i} d\kappa = 0$, $i = 0,1$. This implies that
$\int G d\kappa = 0$.

The results obtained above can be summarized as fol-
lows. The distribution function in the τ scale satisfies Eq.
(8). To first order in δ, its solution is given by

$$f^1_M = f^1_{M_a}(\kappa) n(r,t) + \delta f^1_{M_b} \cdot \nabla n,$$ (15)

where

$$f^1_{M_i}(\kappa) = f^1_M(\kappa) + \delta f_{M_i}(\kappa).$$

This result is the density gradient expansion which has
previously been a priori assumed for the distribution func-
tion. The use of Eq. (15) into Eq. (6) yields a diffusion-
type equation for the density

$$d_t n = - (v_d - v_{dR}) \cdot \nabla' n + D \cdot \nabla'\nabla' n,$$ (16)

where $v_d - v_{dR}$ is the effective drift velocity, and D is the
diffusion tensor under uniform field condition at the value of
the local field. v_{dR} is the contribution to the drift velocity
resulting from the fact that $\int I(f) d\kappa \neq 0$. These quantities
are defined as

$$v_d = \int v f_{M_a} d\kappa, \quad v_{dR} = \delta \int I(f^1_{M_a}) d\kappa,$$

$$D = - \delta \int v f^1_{M_b} d\kappa.$$

These coefficients depend on the applied field through the
f_M's. They can be tabulated as a function of field by numeri-
cally solving for the f_M's and using the above equations.
Once these coefficients have been evaluated, Eq. (16) may
be used to describe the evolution of the carriers. Thus, in the
time scale, the above results correspond to nonequilibrium
diffusion theory. v, v_r, and v_m can be obtained at t_{j+1} using
Eq. (3). With this information, Eqs. (2) are determinate at

t_{j+1} and can then be used to determine the state S_1 at t_{j+2}.

A more accurate expression than given above for the
distribution in first order ($f^1_{M_1}$) can be obtained by explicit-
ly taking into account the space-time variation of the electric
field. That is, instead of Eq. (4), let

$$f(\kappa,r,t) = f^1_M[\kappa,n(r,t), E(r,t)].$$

Following the steps subsequent to Eq. (4), an expression for
$f^1_{M_1}$ is obtained that in first order ($f^1_{M_1}$) is proportional to
the space and time derivatives of the electric field.[28] With
this approach, no specific form need be assumed a priori for
the distribution function.[29,30] Moreover, a similar procedure
can also be used to obtain more accurate expressions for the
distribution in the S_2 and S_3 states (see below). This exten-
sion of the theory presented is not going to be discussed
further.

B. The S_2 state (defined for times $\sim v_\epsilon^{-1}$)

In this case, Eqs. (2a), (2b), and the equation for
$f_M = f^2_M$ in the τ_ϵ time scale are used to describe the system.
The procedure for obtaining the equation for f^2_M follows
along the same lines as the procedure for f^1_M (Sec. III A).
In this case, the change in scale is accomplished by the rela-
tion

$$f(\kappa,r,t) = f^2_M[\kappa,n(r,t),\bar{\epsilon}(r,t)].$$ (17)

That is, in the τ_ϵ scale, the space-time dependence of the
distribution is taken to result from changes in the density
and mean energy. Note that f^2_M changes in two characteris-
tic time scales, τ and τ_ϵ. From Eq. (17), the changes in f
can be written as

$$\partial_t f = \partial_n f^2_M \partial_t n + \partial_{\bar{\epsilon}} f^2_M \partial_t \bar{\epsilon},$$ (18a)

$$\nabla_r f = \partial_n f^2_M \nabla n + \partial_{\bar{\epsilon}} f^2_M \nabla \bar{\epsilon},$$ (18b)

$$\nabla_\kappa f = \nabla_\kappa f^2_M.$$ (18c)

The time derivative of the density and mean energy may be
eliminated from Eq. (18a) by using Eqs. (6) and (2b) re-
written in the form

$$\partial_t \bar{\epsilon} = n^{-1} \left(- \int \partial_n f^2_M \epsilon \, v \, d\kappa \cdot \nabla n - \int \partial_{\bar{\epsilon}} f^2_M \epsilon \, v \, d\kappa \cdot \nabla \bar{\epsilon} \right.$$

$$\left. + qE \cdot \int v f^2_M \, d\kappa + \int \epsilon I(f^2_M) d\kappa \right).$$ (19)

[The term proportional to $\partial_t \ln n$ is assumed to be small and
hence has been neglected in Eq. (19).] Note that in this case,
the average velocity u is obtained from

$$n u = \int v f^2_M \, d\kappa.$$ (20)

After placing Eqs. (6), (19), and (18) in Eq. (1), the fol-
lowing equation is obtained for the distribution function:

$$\partial_n f^2_M \left(- \int \partial_n f^2_M v \, d\kappa \cdot \nabla n + \int I(f^2_M) \partial\kappa \right)$$

$$+ \partial_{\bar{\epsilon}} f^2_M n^{-1} \left(- \int \partial_n f^2_M \epsilon \, v \, d\kappa \cdot \nabla n \right.$$

$$\left. - \int \partial_{\bar{\epsilon}} f^2_M \epsilon \, v \, d\kappa \cdot \nabla \bar{\epsilon} + qE \cdot \int v f^2_M \, d\kappa \right.$$

$$- \int \epsilon I(\,f^{\,2}_{M}\,)d\kappa\Big) + \mathbf{v}\cdot\nabla n\partial_n f^{\,2}_{M} + \mathbf{v}\cdot\nabla\bar{\epsilon}\,\,f^{\,2}_{M}$$

$$+ (qE\cdot\mathbf{f} + \nabla_\kappa f^{\,2}_{M} - I(\,f^{\,2}_{M}\,) \qquad \qquad (21)$$

To expedite the algebra in obtaining a solution to Eq. (21), results obtained for $f^{\,2}_{M}$ [see Eq. (15)] will be used as a guide. That is, let $f^{\,2}_{M}$ be expressed to first order in spatial gradients, by

$$f_{M}(\kappa,n,\bar{\epsilon}) = f^{\,2}_{M}(\kappa,\bar{\epsilon})n + f^{\,2}_{M}(\kappa,\bar{\epsilon})n$$

$$+ f^{\,2}_{M}(\kappa,\bar{\epsilon})\cdot\nabla n + f^{\,2}_{M}(\kappa,\bar{\epsilon})\cdot\nabla\bar{\epsilon}$$

$$(22)$$

The objective for the rest of this section is to arrive at the lowest-order solution for $f^{\,2}_{M}$. Higher-order approximations and the effect of the gradient terms are to be considered in the future. Thus, only the first term in this expansion will be retained. The equation for $f^{\,2}_{M}$ is found to be

$$f^{\,2}_{M}\Big(-\int I(\,f^{\,2}_{M}\,)d\kappa\Big)$$

$$+ \partial_{\bar{\epsilon}}f^{\,2}_{M}\Big(qE\cdot\int \mathbf{v}f^{\,2}_{M}\,d\kappa + \int \epsilon I(\,f^{\,2}_{M}\,)d\kappa\Big)$$

$$+ (q/\hbar)E\cdot\nabla_\kappa f^{\,2}_{M} = I(\,f^{\,2}_{M}\,). \qquad (23)$$

This is a nonlinear equation for $f^{\,2}_{M}$. Neglecting the first term (assuming that the effective carrier gain integral is small), and using the following definitions:

$$\mathbf{u} = \mathbf{u}_\epsilon = \mathbf{u}_\epsilon(\bar{\epsilon}) = \int \mathbf{v}f^{\,2}_{M}\,d\kappa, \qquad (24a)$$

$$v_{\bar{\epsilon}}\bar{\epsilon} = \int \epsilon I(\,f^{\,2}_{M}\,)d\kappa. \qquad (24b)$$

Equation (23) becomes

$$(qE\cdot\mathbf{u} + v_\epsilon\bar{\epsilon})\,\partial_{\bar{\epsilon}}f^{\,2}_{M} - (q/\hbar)E\cdot\nabla_\kappa f^{\,2}_{M} = I(\,f^{\,2}_{M}\,). \qquad (25)$$

At this level of approximation to $f^{\,2}_{M}(\kappa,n,\bar{\epsilon})$, Eqs. (25), (6), and (19) form the closed set of equations that describes the evolution of the system. $f^{\,2}_{M}$ is made to satisfy the following normalization conditions:

$$\int f^{\,2}_{M}\,\epsilon(\kappa)d\kappa = \bar{\epsilon}, \qquad (26a)$$

$$\int f^{\,2}_{M}\,d\kappa = 1. \qquad (26b)$$

The solution to Eqs. (25) and (26) can be obtained as follows. Performing a change of variables from $(\bar{\epsilon},\kappa)$ to $(\omega,\xi,\kappa_\perp)$, where

$$\kappa = \kappa_\parallel \mathbf{a}_\parallel + \kappa_\perp$$

($\mathbf{a}_\parallel$ is a unit vector parallel to E),

$$\xi = \hbar\kappa_\parallel - \bar{\epsilon}/u_\epsilon,$$

$$\omega = \epsilon/u_\epsilon,$$

$$\kappa_\perp = \kappa_\perp,$$

and, using the chain rule,

$$\partial_\epsilon\Big(\frac{\partial}{\partial_\epsilon}\Big) + \partial_\epsilon\frac{\partial}{\partial_\epsilon} = -\frac{1}{u_\epsilon}\partial_\xi + \frac{1}{u_\epsilon}\partial_\omega.$$

[to zeroth order in $\partial_{\bar{\epsilon}}u_\epsilon(\bar{\epsilon})$],

$$\partial_{\bar{\epsilon}}\quad f_M d\kappa\,.$$

Eq. (25) becomes

$$qE_{eq}\partial_\omega f^{\,2}_{M} + q(E_{eq} - E)\,\partial_{\bar{\epsilon}}f^{\,2}_{M} = I(\,f^{\,2}_{M}\,),$$

$$(27)$$

where

$$qE_{eq}\quad v_\epsilon\bar{\epsilon}/u_\epsilon = v_\epsilon\omega. \qquad (28)$$

For $\delta = (E_{eq} - E)/E_{eq}$ small (or $f^{\,2}_{M}$ a slow varying function of ω), the lowest-order solution to Eq. (27) satisfies the following equation:

$$qE_{eq}\partial_\omega f^{\,2}_{M} = I(\,f^{\,2}_{M}\,). \qquad (29)$$

This equation has the form of a steady-state BTE with qE_{eq} as the source. It is equivalent to Eq. (10) that arises in connection with the description of the S_1 state. Thus, to lowest order the macroscopic-kinetic distribution function obeys a steady-state BTE in an equivalent field. This observation has a physical interpretation. The actual field E appears as a source term in the moment equations and as such causes changes in the state S_2. Since the equations describe the evolution of S_2 in their characteristic time scales, variations in E are "filtered" by the equations; that is, as far as changes in S_2 are concerned. Thus, it is the "filtered" field which the state really "sees." This "filtered" field is the equivalent field in Eq. (29).

Equation (29) can be solved numerically with E_{eq} as a parameter. By requiring that

$$\bar{\epsilon} = \int \epsilon(\kappa)f^{\,2}_{M}\,d\kappa,$$

a table for $\bar{\epsilon}$ vs E_{eq} can be generated. Moreover, using Eqs. (3a) and (24), all unknown variables/parameters in Eqs. (2a) and (2b) can be determined as functionals of E_{eq} or equivalently $\bar{\epsilon}$. In this fashion, $v = v(\bar{\epsilon})$, $v_\epsilon = v_\epsilon(\bar{\epsilon})$, and $u = u_\epsilon(\bar{\epsilon})$. The system of equations describing S_2 is closed.

C. The S_3 state (valid for times $\sim v_m^{-1}$)

In this case, Eqs. (2a)–(2c) and the equation for $f_M = f^{\,3}_{M}$ in the τ_m time scale are used in the description of the system. In the spirit of Eqs. (4) and (17), the distribution function is assumed to depend in space and time as follows:

$$f(\kappa,r,t) = f^{\,3}_{M}[\kappa,n(r,t),\bar{\epsilon}(r,t),\bar{\kappa}(r,t)].$$

Although obtaining an equation for $f^{\,3}_{M}$ is straightforward, its solution is more difficult to find than for cases S_1 and S_2. This stems from the fact that, even in zeroth order, it is an equation in three variables $(\bar{\epsilon},\bar{\kappa},\kappa)$.

In this paper, instead of proceeding to find an equation for $f^{\,3}_{M}$ and obtaining its solution, an approximate expression for $f^{\,3}_{M}$ is presented. A more complete theory (in essence, a more rigorous derivation of the expression present-

ed) will be the subject of a future paper

In all cases of interest, the nonequilibrium macroscopic equations are solved using numerical methods. With those methods, the field E in each time step is taken to be constant. Thus, the solution for f_M in a time step corresponds to the approach to equilibrium of an initial distribution in the presence of a field (i.e., an initial value problem in each time step). From the discussions in the previous sections, it is known that after a sufficient time, the "initial distribution" will evolve into f_M (if the time step is long enough). Thus, an approximate expression for f_M can be obtained by assuming that this evolution can be modeled by a relaxation process. Let the macroscopic state S, and f_M be known at time t, when the field is $E(r,t)$. Note that the field does not change in the interval (t, t_{+1}) and that the distribution $f_M(t)$ (i.e., the distribution at time t) is not the equilibrium distribution for the field $E(r,t)$. Thus, in spirit of the above discussion, the distribution at time $t + \rho$ (where ρ is a continuous variable) can be written as

$$f_M(t + \rho) = [f_M(t) - f_M(t + \rho)] e^{...}$$

$$+ f_M(t + \rho) \quad \text{for } \rho > 0. \quad (30)$$

where ν_m is the average momentum exchange frequency in the interval (t, t_{+1}); $\nu_m \rho = \int_0^\rho \nu_m(\rho) d\rho$. That is, f_M approaches f_M exponentially, due to the relaxation of the fast component $(f_M - f_M)$ resulting from momentum transfer at an average rate ν_m. The distribution at the end of the interval is found by letting $\rho = \Delta t$ in Eq. (30), once $f_M(t_{+1})$ is found. This procedure is to be repeated at each time interval. Note that to implement this approach f_M must also be known at each step. This problem has been discussed in Sec. III B.

A simple alternative to Eq. (30) is to let f_M be equal to f_M in the calculation of the unknown variables in the macroscopic Eqs. (2a)-(2c). This substitution leads to the phenomenological equations proposed by Shur for space-independent conditions.

IV. EXAMPLE: THE RESPONSE OF A HOMOGENEOUS CONCENTRATION OF ELECTRONS IN GaAs TO A STEP CHANGE IN ELECTRIC FIELD

In this section, the response of a homogeneous concentration of electrons in GaAs to a step change in electric field is investigated using the theory developed in Sec. III. For the sake of simplicity, it is assumed that there is no particle gain; that is, $n(r,t) = \text{const}$. Moreover, a single-valley model has been used for the band structure. As mentioned in Sec. I, this model has severe limitations, particularly at the values of field under consideration. However, the objective of this example is to illustrate the application of the theory presented in the previous section with a "model" calculation. The evolution of the electrons is discussed in the context of the S_1 time scales. This is dictated by the time scale of the applied field. For this example, Eqs. (2a)-(2c) reduce to

$$\partial_t \bar{\epsilon} = - \nu_\epsilon (\bar{\epsilon} - \bar{\epsilon}_0) + quE, \quad (31a)$$

$$\partial_t \bar{p} = - \nu_m \bar{p} + qE, \quad (31b)$$

where $\bar{\epsilon}_0$ is the mean energy corresponding to the lattice temperature, $\bar{p} = \hbar\bar{\kappa}$, and $\nu_i, i = \epsilon, m$, are obtained from Eqs. (3b) and (3c) with $f = f_M$.

These equations have been solved numerically using finite difference techniques. At the jth time step, the mean energy $\bar{\epsilon}(j)$ and average momentum $\bar{p}(j)$ are obtained from the discrete equations, given their values and the rates at the previous time step $j-1$. After substituting in Eqs. (3b) and (3c) for f_M [Eq. (30)], the rates at the jth time step are obtained from

TABLE I. Rate coefficients for electrons in GaAs computed in the S_2 description as a function of E_{eq}, or equivalently, as functions of $\bar{\epsilon}$.

E_{eq} (kV/cm)	$\bar{\epsilon}$ (eV)	$(\bar{\epsilon} - \bar{\epsilon}_0)\nu_{\bar{\epsilon}} (10^{10}$ eV/s)	$\nu_m(\epsilon)(10^{12}$ s$^{-1})$
0.1	0.319	0.0116	2.292
0.2	0.0336	0.04216	2.684
0.3	0.03475	0.0906	2.796
0.4	0.0357	0.1566	2.894
0.5	0.0363	0.239	2.933
0.6	0.0373	0.3413	2.95
0.8	0.0388	0.588	3.046
1.0	0.0405	0.8964	3.103
1.1	0.0415	1.062	3.13
1.2	0.043	1.254	3.187
1.3	0.0444	1.453	3.216
1.4	0.0458	1.663	3.243
1.5	0.047	1.886	3.285
1.6	0.0476	2.112	3.317
1.7	0.0481	2.343	3.339
1.8	0.0492	2.343	3.362
2.0	0.0559	2.892	3.517
2.2	0.062	3.487	3.534
2.5	0.070	4.285	3.638
5.0	0.2017	9.3	5.714
10.0	0.3127	12.53	12.53
20.0	0.3705	21.86	20.39
30.0	0.408	31.98	26.64
40.0	0.4412	42.6	31.92
50.0	0.4655	49.5	39.62
60.0	0.4975	59.22	44.25
70.0	0.5229	68.48	49.04

$$\nu_i(j) = [\nu_i(j-1) - \nu_i^{(0)}(j)]e^{-\nu_m \Delta t} + \nu_i^{(0)}(j),$$

$$(32)$$

where $i = \epsilon, m$, and the superscripts correspond to rates in the S_2 scales (see Sec. III C). The $\nu_i^{(0)}$'s are obtained from Eqs. (3b) and (3c), with $f = f_M^2$. f_M^2 is obtained using Monte Carlo methods. The values for the $\nu_i^{(0)}$'s obtained from the Monte Carlo model are listed in Table I as a function of mean energy.

In these calculations, ν_{m_j} has been approximated by $\nu_m(j-i)$. This is the momentum exchange frequency at the beginning of the interval. Thus, with $\bar{\epsilon}(j-1)$, $\bar{p}(j-1)$, and $\nu_i(j-1)$ given, the values of $\bar{\epsilon}(j)$, $\bar{p}(j)$, and $\nu_i(j)$ are obtained by solving Eqs. (31a), (31b), and (32). This procedure is repeated at each time step.

The evolution of the mean energy and average velocity of the electrons in GaAs subjected to a step change in electric field is shown in Figs. 1 and 2. Two cases are shown. These correspond to two different time dependencies of the electric field (see Fig. 3). The initial field is kept constant for a time
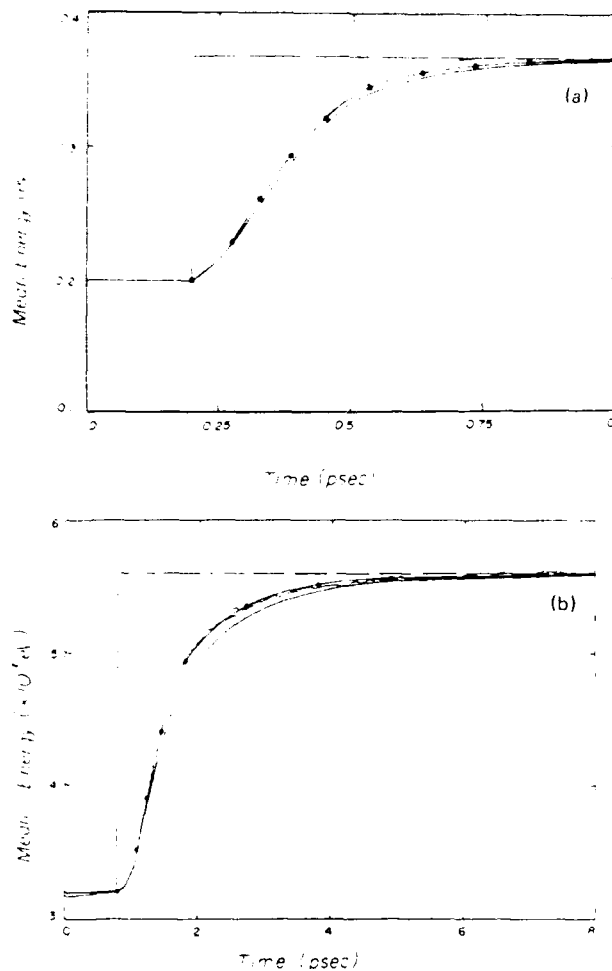
FIG. 1. Evolution of the electron mean energy as a consequence of a step change in the applied field (see Fig. 3). On the figures, the large dot, solid, long dash, and small dot lines correspond to the response obtained with the S_1S_2 and S_1 descriptions and Monte Carlo simulation, respectively. (a) and (b) correspond to field changes shown in Figs. 3(a) and 3(b), respectively.
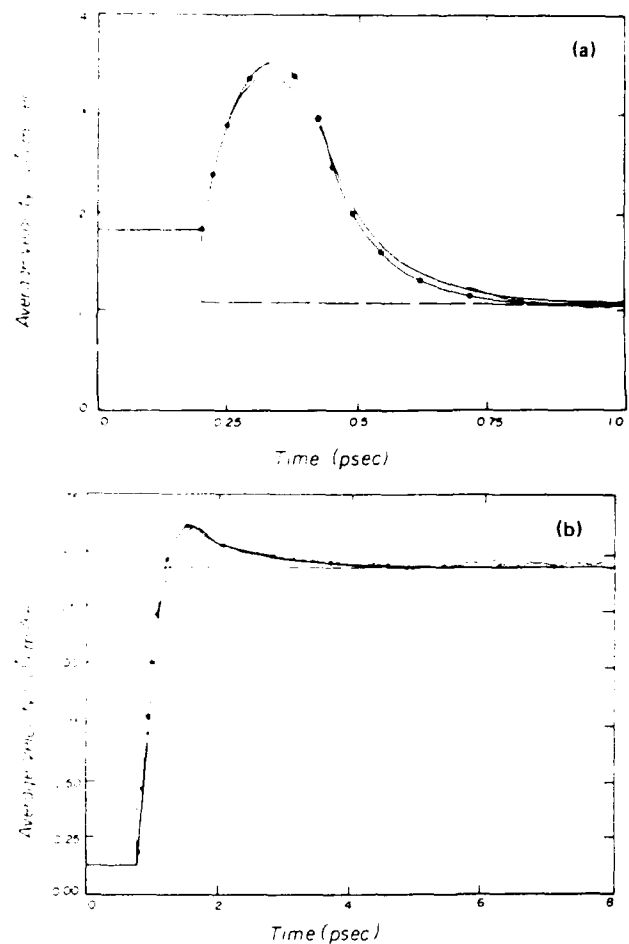
FIG. 2. Evolution of the average velocity of the electrons as a consequence of a step change in the applied field (see Fig. 3). The line symbols correspond to those used in Fig. 1. (a) and (b) correspond to field changes shown in Figs. 3(a) and 3(b), respectively.

such that the electrons have attained equilibrium with the field by the time the field begins to change. Also shown in Figs. 1 and 2 are the results obtained using: (a) Monte Carlo methods, with a three-valley model[32]; (b) Eqs. (31a) and (31b) with rates determined from the S_2 state (i.e., by letting $f_M = f\,^2_M$); and (c) the S_1 state approximation.

The differences between the results obtained with the S_3 description and the Monte Carlo in simulation in Fig. 2(a) arise primarily from the fact that the S_3 description uses a single-valley representation. For such high fields [see Fig. 3(a)] intervalley scattering dominates the scattering process of electrons in GaAs. It causes the slower approach of the average velocity (relative to the S_3 description) to the equilibrium state. For lower fields [see Fig. 3(b)], a very small fraction of the electrons gain sufficient energy to populate the upper valleys through intervalley scattering. Because of this, the response of the carrier distribution to the change in electric field is not determined by intervalley scattering [as it is at higher fields; see Figs. 2(a) and 2(b)]; and thus, it is faster than at higher fields. At lower fields, the single-valley nonequilibrium moment theory results for the mean energy are in very good agreement with the Monte

Carlo results [see Fig. 2(b)]. However, the results for the average momentum are observed to relax slower than the Monte Carlo results. This is also in part due to the fluctuations in the Monte Carlo results at low fields for the macroscopic rates obtained with the S_2 description. Presently, a three-valley S_3 model is being implemented. The detailed multivalley effect on nonequilibrium dynamics of electrons will be discussed in the future paper. The evolution of the system from the initial equilibrium state (I) to the final equilibrium state (F) is displayed in ($\bar\varepsilon, u$) space in Fig. 4. The fast transient (nonequilibrium) behavior obtained with the S_3 approximation is clearly contrasted with those obtained from the S_1 approximation (which in essence yields an evolution through a series of equilibrium states). As expected, for fields changing in time scales $< v_c^{-1}$, a description in terms of S_1 is not satisfactory.

V. CONCLUDING REMARKS

Nonequilibrium descriptions of the dynamics of electrons in a semiconductor under the influence of space-time varying fields have been presented. These descriptions are valid in different macroscopic space-time scales which are
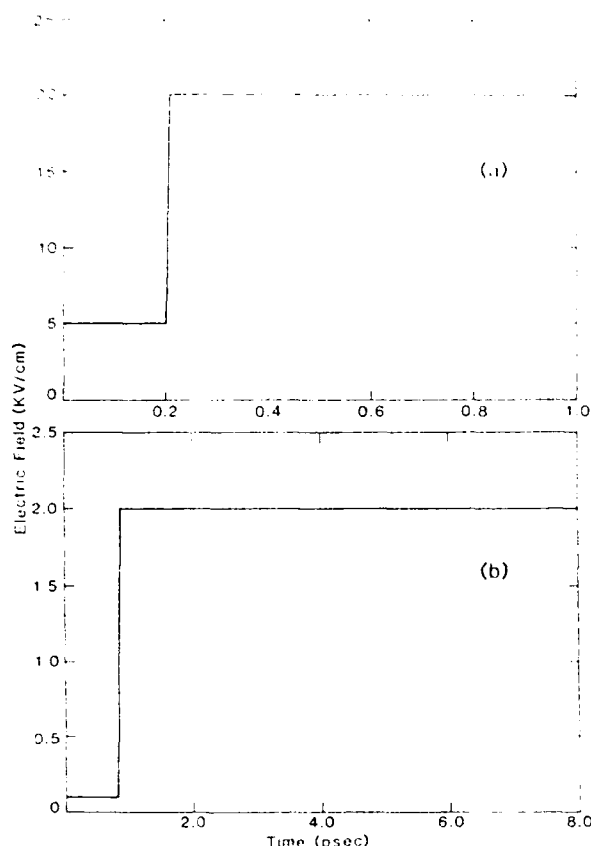
FIG. 3. Time dependence of the applied field corresponding to the results shown in Figs. 1 and 2: (a) high-field and (b) low-field cases.

determined from the characteristic scales of the moment equations. The results that have been presented in this paper correspond to the lowest-order solutions of these description. In the fastest scale (S_3), these lowest-order results have been shown to be in reasonable agreement with those obtained from a kinetic description. A number of issues remain to be addressed. Among these issues are (a) the (more) quantitative description of the S_3 state, (b) the relative importance of higher order terms in the expansions of f_M and of faster time scales (S_4 or higher), and (c) the relationship between a description in terms of S_1 and a modal decomposition of the distribution function. These issues will be discussed in a future publication.
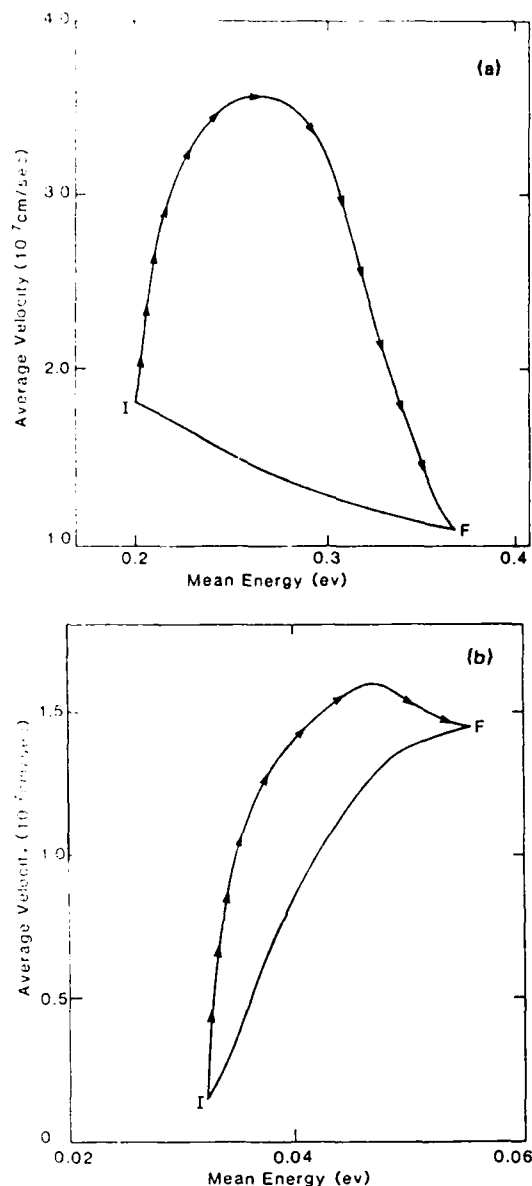
FIG. 4. Phase-space plot of the evolution of the electron assembly. The letters I and F correspond to the initial and final states. The arrows indicate the direction of evolution. The solid line with arrow corresponds to the response in the S_1 description; the line without arrows corresponds to the S_1 description (a) and (b) correspond to field changes shown in Figs. 3(a) and 3(b), respectively.

[1] R. Peieris, in Lecture Notes in Physics 31: Transport Phenomena, edited by J. Ehlers, K. Hepp, and H. A. Weidenmuller (Springer, Berlin, 1974).
[2] E. Cohen and W. Thirrign, Eds., The Boltzmann Equation, Acta Phys. Austriaca Supl. X (Springer, Berlin, 1973).
[3] P. Price, Solid State Electron. 21, 9 (1978).
[4] H. D. Rees, J. Phys. Chem. Solids 30, 643 (1969).
[5] C. Hammar, J. Phys. C 6, 70 (1973).
[6] C. Jacoboni and L. Reggiani, Rev. Mod. Phys. 55, 645 (1983).
[7] W. Fawcett, A. D. Boardman, and S. Swain, J. Phys. Chem. Solids 31, 1963 (1970).
[8] S. Chapman and T. G. Cowling, The Mathematical Theory of Non-Uniform Gases (Cambridge University Press, Cambridge, 1961).
[9] H. Cran , Mathematical Methods of Statistics (Princeton University Press, Princeton, 1946).
[10] M. Friscourt, P. Rolland, A. Cappy, E. Constant, and G. Salmer, IEEE Trans. Elec. Devices ED-30, 223 (1983).
[11] A. Ghis, E. Constant, and B. Boittiaux, J. Appl. Phys. 54, 214 (1983)

[12] F. A. Buot and J. Frey, in The Physics of Submicron Structures, edited by H. L. Grubin, K. Hess, G. J. Iafrate, and D. K. Ferry (Plenum, New York, 1984), p. 77.
[13] H. L. Grubin, D. K. Ferry, G. Iafrate, and J. R. Barker, in VLSI Electronics Vol. 3, edited by N. G. Einspruch (Academic, New York, 1982), p. 197.
[14] T. J. Mahoney and J. Frey, J. Appl. Phys. 48, 781 (1977).
[15] W. Hansch and M. Miura-Mattausch, J. Appl. Phys. 60, 650 (1986).
[16] E. M. Conwell and M. O. Vassell, Phys. Rev. 166, 797 (1968).
[17] H. Frohlich, Proc. R. Soc. London A 188, 521 (1947).
[18] R. Stratton, Proc. R. Soc. London A 246, 406 (1958).
[19] K. Blotekjar, IEEE Trans. Elect. Devices ED-17, 38 (1970).
[20] M. S. Shur, Electron Lett. 12, 615 (1976).
[21] B. Carnez, A. Cappy, A. Kaszynski, E. Constant, and G. Salmer, J. Appl. Phys. 51, 784 (1980).
[22] E. Kunhardt, C. Wu, and B. Penetrante, Phys. Rev. A 37, 1654 (1988).
[23] H. Grad, Phys. Fluids 6, 147 (1963).

I. S. ...et, Phys. Fluids **6**, 218 (1963).

F. R. Bass... and D. Ferry, Solid State Electron. **23**, 519 (1980).

N. N. B...g... in *Studies in Statistical Mechanics*, edited by J. deBoer and G. E. Uhlenbeck (Interscience, New York, 1962).

I. N. F...man, J. Math. Phys. **4**, 410 (1963).

E. E. Kunhardt, Bull. Am. Phys. Soc. **30**, 170 (1985).

K. K. Thornber, IEEE Trans. Electron. Devices Lett. **EDL-3**, 69 (1982).

N. I. Alexander, A. P. Napartovich, and A. N. Starostin, Sov. J. Plasma Phys. **6**, 618 (1980).

C. W. Gear, *Numerical Initial Value Problems in Ordinary Differential Equations* (Prentice Hall, New York, 1971).

M. Cheng and E. E. Kunhardt, J. Appl. Phys. **63**, 2322 (1988).

IV. ELECTRON ENERGY DISTRIBUTIONS, TRANSPORT PARAMETERS, AND RATE COEFFICIENTS IN GaAs

I. INTRODUCTION

Under certain conditions, the behavior of an assembly of electrons or holes in a semiconductor, and influenced by space-time varying fields, is described by the time-dependent semiclassical density distribution, $f(\mathbf{k},\mathbf{r},t)$, in configuration $\mathbf{r}$ and momentum $(\mathbf{k})$ space.[1] In multivalley semiconductors with a different effective mass in each valley, a description of carrier behavior in terms of a single distribution function may not be adequate.[1] Moreover, transport parameters and rate coefficients that appear in a single-valley hydrodynamic model do not reflect in such cases the dynamics of the carriers. This is especially true for values of applied field where intervalley scattering is significant. In these cases, the transport parameters not only depend on the transport properties, but also on the rate coefficients. For example, drift velocity, defined as the time rate of change of the center of mass of a group of electrons,[2] will depend on the averaged intervalley scattering rate. This is due to the fact that carriers moving with the group are scattered into valleys with different masses (and consequently different dynamics) resulting in a change in the center of mass without (necessarily) any transport. Thus, in these situations, a multidistribution description of the behavior of the carriers is desirable at both the kinetic [$f_\alpha(\mathbf{k},\mathbf{r},t)$, where α denotes a particular valley] and hydrodynamic (in terms of moments of the f_α's) levels.

The distribution function, transport parameters, and rate coefficients in each valley can, in principle, be obtained from Monte Carlo simulation[3,6] or from solution of the Boltzmann transport equation (BTE) by either iterative[7–9] or analytical[10–12] techniques. At present, the Monte Carlo approach has a number of advantages over the BTE approach: it is relatively easy to implement a six-dimension ($\mathbf{k},\mathbf{r}$) space simulation; it can be easily modified to accommodate any number of interactions between the carriers and the background; and it provides considerable physical insight into the behavior of the carriers, including fluctuation phenomena.

In the Monte Carlo approach, the accuracy of the results depends (a) in transient situations, on the number of electrons used in the simulation, and (b) in steady state, on the total number of scatterings. A major drawback of the Monte Carlo approach is that the simulation takes a considerable amount of computer time, even when very few electrons are used. This becomes more serious when simulating, for example, the behavior of electron in a multivalley semiconductor subjected to low electric field. In this case, a very small fraction of the electrons gain sufficient energy to populate the upper valleys through intervalley scattering. For example, in GaAs, less than 2% of the electrons are in the X valleys when $E = 20\,\text{kV/cm}$ (see Fig. 4). Thus, to obtain an accurate representation of the behavior of the electrons in the X valleys, it is necessary to use in the order of tens of thousand electrons in the Monte Carlo calculation. Such a large number of electrons make this approach, in some cases, prohibitive.

To simplify the computational aspects of the Monte Carlo approach, Rees[9,13] introduced the concept of self-scattering. However, when the carrier scattering rates are increasing functions of energy, standard implementations of this concept leads to a very large number of fictitious scattering events along the carrier trajectories, and thus results in a further increase in the computation time. We have developed a technique for reducing the number of self-scattering events. Consequently, for a given CPU (central processing unit) time, more test particles can be used in the simulation. This results in a reduction in the fluctuation of the calculated quantities. This technique is discussed in the next section in the context of two generic time dependencies of the applied field, namely, dc and a step change. In Sec. IV, results from simulations of the steady-state behavior of electrons in a three-valley model of GaAs are presented. Concluding remarks are given in Sec. V.

II. THE MONTE CARLO TECHNIQUE

In the Monte Carlo approach for simulating the behavior of carriers in semiconductors and influenced by space-time varying fields, the initial distribution of carriers [$f(\mathbf{k},\mathbf{r},0)$] is specified. An initial number of test carriers are then selected that are representative of this distribution, and their evolution simulated using statistical methods.[2–6,13] In this paper, it is assumed that energy ϵ of an electron is related to the wave-vector $\mathbf{k}$ through the equation[4,14]

$$h^2k^2/2m = \epsilon(1 + \alpha\epsilon) , \tag{1a}$$

where h is the Planck constant divided by 2π, m is the effective mass of the electron with zero energy in the valley, and α is the nonparabolicity parameter. m and α depend on the valley in which the electron is found. Equation (1a) represents a nonparabolic energy band with spherical constant surfaces and a scalar effective mass m. For a nonparabolic energy band with ellipsoidal constant energy surface, the $\epsilon - \mathbf{k}$ relation is given by

$$\frac{h^2}{2}\left(\frac{k_l^2}{m_l} + \frac{k_t^2}{m_t}\right) = \epsilon(\mathbf{k})[1 + \alpha\epsilon(\mathbf{k})] , \tag{1b}$$

where m_l and m_t are the longitudinal and transverse components of the effective mass tensor,[15,16] and k_l and k_t are the longitudinal and transverse components of the wave vector of the electron. For the values of field of interest, Eq. (1) represents a good approximation to more accurate representations for the band structure. Moreover, the use of Eq. (1) in the trajectory equations is consistent with the formulation of scattering rates as functions of energy, which assumes an energy-momentum relation given by Eq. (1).

Note that it is sufficient to only discuss the case of an energy band with spherical constant energy surfaces [Eq. (1a)]. The resulting equations are also valid for the ellipsoidal case [Eq. (1b)] if m is replaced with free-electron mass, and the wave vector and electric field are replaced with the Herring–Vogt transformed values.[15,16]

The flight of an electron between scattering events is calculated using the equation of motion ($h\,\partial_t\mathbf{K} = q\mathbf{E}$) and either Eqs. (1a) or (1b). The time t_s between scattering events is determined from the equation[2,4]

$$R_1 = 1 - \exp\left(-\int_0^{t_s} v_T[\epsilon(t)]dt\right), \tag{2}$$

where R_i is a uniformly distributed random number in the interval $[0,1]$, and v_T is the total scattering rate, which is a function of the time-dependent electron energy.

The integral in Eq. (2) cannot, in general, be evaluated analytically. To overcome this difficulty, a fictitious scattering event is introduced such that the "new" total scattering rate v'_T would be constant.[3,4] This v'_T is taken to be greater or equal to the minimum constant that makes $v_{self}(\epsilon)$ positive for all ϵ in the expression [see Fig. 1(a)]

$$v'_T = v_{self}(\epsilon) + v_T(\epsilon) . \tag{3}$$

$v_{self}(\epsilon)$ is the scattering rate for the fictitious scattering mechanism. This process causes no changes in the properties of the electron along the trajectory. That is, the state $\mathbf{k}'$ of an electron after a self-scattering event is taken to be equal to its state $\mathbf{k}$ before the event. With v_T in Eq. (2) replaced by v'_T (which is constant), the integral in Eq. (2) is evaluated, and the duration of the free flight t_s is found. The procedure for determination of the scattering mechanism and direction has been described in the other papers.[2,4] From Eq. (3), note that the number of self-scattering events is always much greater than the number of real scattering events. To reduce the number of self-scattering events resulting from the use of Eq. (3), a step-shaped total scattering rate $v_T^s(\epsilon)$ has been

proposed.[2] $v_T^s(\epsilon)$ is given by

$$v_T^s(\epsilon) = \begin{cases} v_{T1}, & \epsilon < \epsilon_1 \\ v_{T2}, & \epsilon > \epsilon_1, \end{cases}$$

where ϵ_1 is a suitable boundary between two energy regions with constant scattering rates, namely v_{T1} and v_{T2} [see Fig. 1(b)]. The constants v_{T1} and v_{T2} are constant total scattering rates which include self-scattering. t_s is then obtained from Eq. (3), as discussed in Ref. 2.

The step-shaped total scattering rate, $v_T^s(\epsilon)$, outlined above does not significantly decrease the simulation time unless more steps are used. On the other hand, the use of more steps cause difficulty in the implementation of the scheme. This is because situations in which an electron travels across two or more energy regions without suffering any scattering have to be considered.

To significantly reduce the number of self-scattering events while keeping the implementation of the scheme relatively simple, we propose the following scheme: (a) change the integration variable in Eq. (2) from time t to momentum k; (b) use a quadratic polynomial to represent the total scattering rate (including self-scattering) v_T^q; and (c) use the energy-momentum relation, Eq. (1), to carry out the integration.

Following this procedure, let $v_T(\epsilon)$ in Eq. (2) be given by v_T^q; that is,

$$v_T^q(\epsilon) = A + B\epsilon(1 + \alpha\epsilon) , \tag{4a}$$

and using Eq. (1),

$$v_T^q(k) = A + B(h^2k^2/2m) , \tag{4b}$$

where A and B are constants, which are chosen from the requirement that $v_{self}(\epsilon)$ in Eq. (3) must be positive and as small as possible in the energy range of interest [see Fig. 1(c)]. After changing the variables of integration from t to k_z and utilizing Eq. (4) and the equation of motion, Eq. (2) becomes

$$Ah\int_{k_{z0}}^{k_z}\frac{dk_z}{qE} + \frac{Bh^3}{2m}\int_{k_{z0}}^{k_z}\frac{k^2}{qE}\,dk_z = -\ln(1-R_1) , \tag{5}$$

where k_{z0} is the initial value of the longitudinal component of the wave vector $\mathbf{k}$, $k^2 = k_x^2 + k_y^2 + k_z^2$, and we have taken E along the z direction. E in Eq. (5) may be either space-time dependent or constant. The piecewise application of Eq. (4b) in the energy interval of interest results in further reduction of the number of self-scattering events. The resulting total rate v_T^{qs} is further discussed in the next section.

Since space-time simulations are implemented as a series of time intervals in which the field is constant in time,[6,17] it is only necessary to investigate the generic problems of constant and step field variations. These two cases are considered below.

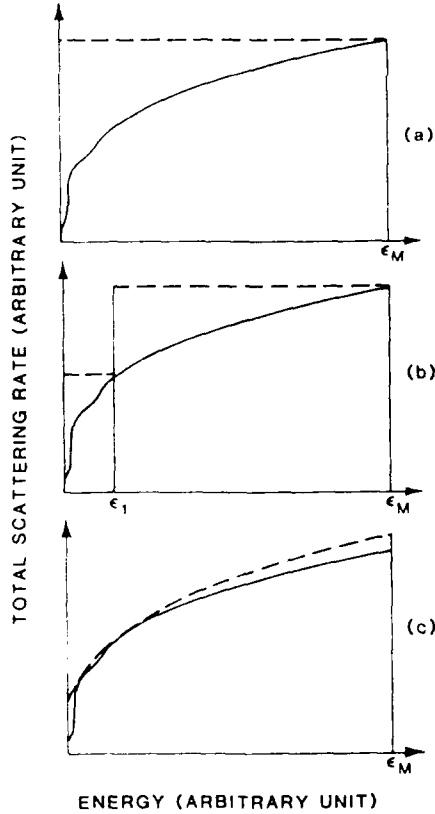1. Static electric field: In this case, Eq. (5) reduces to

FIG. 1. Energy dependence of the total scattering rates. The solid lines represent the total scattering rate $v_T(\epsilon)$. The dashed lines represent (a) a constant total scattering rate v'_T, (b) a step-shaped total scattering rate $v_T^s(\epsilon)$, and (c) a total scattering rate $v_T^q(\epsilon)$ given by Eq. (9a). ϵ_M is a maximum electron energy; ϵ_1 is a suitable boundary between two energy regions with constant scattering rates.

$$k_z^3 + 3\left(k_r^2 + \frac{2mA}{h^2B}\right)k_z + \frac{6mqE}{Bh^3}\ln(1-R_1)$$

$$-\left(\frac{6mA}{h^2B}k_{z0} + 3k_r^2k_{z0} + k_{z0}^3\right) = 0 , \tag{6}$$

where $k_\perp = \sqrt{k_x^2 + k_y^2}$ is the transverse component of the wave vector which is constant during the free flight. Since Eq. (6) has only one real root, it simplifies the determination of k_z at the end of the free flight for a given random number R_1. The duration of the free flight t_1 is then obtained from the equation of motion.

2. Step electric field: The case of a step variation in time of the applied field can be treated in a similar way as for a constant field. Let the applied field be in the z direction, and equal to E_I for $t < t_1$ and E_{II} for $t > t_1$. To determine the state of the electron at the end of a free path, it is necessary to know the location of the free flight relative to that of the step. This gives rise to two situations:

(i) An electron ends its free flight at $t < t_1$ or starts the free flight at $t > t_1$. In these cases Eq. (6) is solved for the longitudinal component of the wave vector k_z at the end of the free path, within $E = E_I$ or $E = E_{II}$, respectively.

(ii) An electron begins its free flight at $t < t_1$ and ends it at $t > t_1$. In this case, the integral in Eq. (5) can be decomposed into two regions (namely, $E = E_I$ and $E = E_{II}$) and integrated to give

$$k_z^3 + 3\left(k_\perp^2 + \frac{2mA}{h^2 B}\right)k_z + \frac{6mqE_{II}}{Bh^3}[\ln(1 - R_1) + C_1 + C_2]$$
$$- \left(\frac{6mA}{h^2 B}k_{z1} + 3k_\perp^2 k_{z1} + k_{z1}^3\right) = 0 .\qquad (7)$$

where

$C_1 = (Ah/qE_L)(k_{z1} - k_{z0}) = A(t_1 - t_0)$,

$C_2 = (Bh^3/2mqE_L)[k_\perp^2(k_{z1} - k_{z0})$

$\qquad + \frac{1}{3}(k_{z1}^3 - k_{z0}^3)]$,

t_0 is the initial time of the free flight, and k_{z1} is the longitudinal component of the wave vector of the electron at $t = t_1$. The longitudinal component of the wave vector k_z at the end of the free flight is determined by solving this cubic equation.

III. ELECTRON ENERGY DISTRIBUTIONS, TRANSPORT PARAMETERS, AND RATE COEFFICIENTS IN GaAs

The Monte Carlo technique presented in the previous section has been implemented to obtain the steady state and step response of electrons in GaAs. As mentioned in the previous section, these are the two generic problems which form the basis for simulations with arbitrary time dependence of the field. In this paper, the steady-state results are discussed. The transient results are to be discussed in a future publication. In Sec. III A, further computational details are given. In Sec. III B, the gain in computation time that has been achieved with the technique presented in Sec. II is illustrated. The results for the distribution function, transport parameters, and rates coefficients are presented in Sec. III C.

A. Further computational details

In the Monte Carlo simulations discussed in this paper, a three-valley model (Γ, L, X) of GaAs has been used. The scattering processes that have been taken into account are polar optical, acoustic phonon, intervalley, and intravalley

scatterings.[24] The intervalley separations $\Delta\epsilon_{\Gamma L}$ and $\Delta\epsilon_{\Gamma X}$ have been taken to be equal to 0.33 and 0.522 eV, respectively.[15] A list of the material parameters that have been used in the simulations is given in Table I. The values given in parentheses are those obtained by Pozela and Reklaitis[19] from best fit to the data of Houston and Evans.[20]

To get an accurate representation of the steady state of electron behavior in each valley, up to 80 000 electrons have been used in the simulations[21] (each electron suffers at least 100 collisions). The sampling procedure has been discussed in detail elsewhere.[6]

B. Illustration of gain in computation time

To illustrate the gain in computational speed that has been achieved with the technique presented, we have carried out comparative simulations with the three total scattering rates discussed in Sec. II, namely, v_T^c, v_T^l, v_T^q, and v_T^{qs}. The rate v_T^{qs} is a modification of v_T^q obtained by piecewise application of Eq. (4b). We have used v_T^{qs} for the rate in the Γ valley in one of our illustrations. Note that v_T^{qs} approaches v_T^l in a given interval when $B \to 0$. Thus, v_T^{qs} is the most general rate that can be used to represent the total scattering rate while still being able to carry out the integration in Eq. (2). This can be considered as the use of quadratic splines for the representation of the actual scattering rate. That is, in the Γ valley, the energy interval is divided into two domains ($\epsilon < \Delta\epsilon_{\Gamma L}$ and $\epsilon > \Delta\epsilon_{\Gamma L}$) and Eq. (4b) is applied to each region. For $\epsilon < \Delta\epsilon_{\Gamma L}$, B is taken to be zero for illustration (see below for further comments). The results are shown in Table II. For the same number of electrons and simulation time (10 ps), the number of real-scattering events are approximately equal. The number of self-scatterings (and total scatterings), however, is considerably different. This also applies to the computation (CPU) time. As seen from Table II, the computation time for the Monte Carlo simulations using v_T^c (constant total scattering) is approximately an order of magnitude and four times larger than the computation times for simulations using v_T^q [Eq. (4)] and v_T^l (piecewise constant total scattering), respectively. Further reductions in the number of self-scatterings were obtained with v_T^{qs} (see Table II).

At 10 kV/cm, the mean energy of electrons in the Γ valley of GaAs is about 0.23 eV below the threshold energy $\Delta\epsilon_{\Gamma L}$. As mentioned in Sec. II, for this mean energy, the electron scattering rate in Γ valley of GaAs is nearly constant and results in a large self-scattering rate with the application of v_T^q for the whole interval. Thus, in Table II, the results for $v_T^q(\epsilon)$ show approximately 200 self-scattering events (more than 50% of total scatterings). This number is reduced to less than 100 self-scattering events with the use of v_T^{qs} as shown in Table II (approximately 30% of total scatterings). The number of self-scattering events is expected to be less if the constants A and B used for $v_T^{qs}(\epsilon)$ in each energy region are optimized by properly partitioning the energy interval. By dividing the total energy interval into more sections and applying to each section an equation of the form of Eq. (4), the coefficient A_j and B_j (where j denotes the jth section) can be chosen to minimize the number of self-scattering.

TABLE I. GaAs material parameters.[a]

Density (g/cm³)	5.36 (5.37)
Sound velocity (cm/s)	5.24 × 10⁵ (5.2 × 10⁵)
Static dielectric constant	12.9
Optical dielectric constant	10.92
LO phonon energy (eV)	0.035.36 (0.0362)
Energy separation (eV)	
Γ-L	0.33
Γ-X	0.522 (0.52)

	Γ(000)	L(111)	X(100)
Nonparabolicity (eV⁻¹)	0.61 (0.62)	0.461 (0.5)	0.204 (0.3)
Effective mass (m*/m₀)	0.063	0.222 (0.17)	0.58
Acoustic deformation potential (eV)	7.0	9.2 (7.0)	9.7 (7.0)

Intervalley phonon energy (eV)	Γ(000)	L(111)	X(100)
Γ(000)	0	0.0278 (0.0299)	0.0299
L(111)	0.0278 (0.0299)	0.029 (0.0299)	0.0293 (0.0299)
X(100)	0.0299	0.0293 (0.0299)	0.0299

Intervalley coupling constant (10⁹ eV/cm)	Γ(000)	L(111)	X(100)
Γ(000)	0	1(0.18)	1
L(111)	1(0.18)	1(0.5)	0.5(0.1)
X(100)	1	0.5(0.1)	0.7(1)

[a] See Refs. 18 and 19.

C. Steady-state behavior of electrons in GaAs

1. Energy distribution functions

To elucidate the physics of the steady-state behavior of electrons in a three-valley model of GaAs we have obtained the energy distribution of the electrons in each valley. These distributions are shown in Fig. 2.

At low and medium fields (below 20 kV/cm) where the population of electrons in the X valleys is not significant, these distributions have similar features as those obtained by Fawcett and co-workers[4,22,23] and Conwell and Vassell.[14] As the field increases from zero, electrons are heated up rapidly due to invariant polar optical phonon scattering[4] and the distribution begins to flatten. However, because of strong intervalley scattering, electrons with energy above the threshold for scattering into the L valleys ($\Delta\epsilon_{\Gamma L}$) are driven into equilibrium with the L distribution. This distribution is nearly a Maxwellian at the lattice temperature. For fields above 10 kV/cm, a population inversion is observed in the Γ valley in agreement with the results of Fawcett and co-workers[4,22,23] and Conwell and Vassell.[15] This inversion is due to the fact that intervalley scattering is nearly isotropic, whereas polar optical scattering is primarily forward. On average, half of the electrons scattered from the L to the Γ valley near the threshold energy $\Delta\epsilon_{\Gamma L}$ lose energy to the field and thus move to energy states below $\Delta\epsilon_{\Gamma L}$. Since intervalley scattering in this range is zero, these electrons represent an "uncompensated" source into these states, thus creating the observed population inversion. This type of distribution is not stable and should lead to collective excitations (plasmons).[24] These excitations, however, are not taken into account in this model. However, in contrast to the two-valley model, the population inversion is not very pronounced so that the plasmon excitation rate should be small.

At higher fields (above 20 kV/cm), electrons in the L valleys (as well as the tail of the Γ distribution) begin to heat

TABLE II. Comparison of computation time for the techniques described in Sec. II. Simulation time is 10 ps. E = 10 kV/cm.

Function for total scattering rate	Number of total scattering for single electron	Number of real scattering for single electron	Number of electrons in simulation	CPU time[a] (min)
Constant total scattering rate v'_T	11 000	150–190	2000	196
Three-level step-shaped total scattering v^s_T	2300	150–190	2000	49
Eq. (4) rate v^4_T	350–390	150–190	2000	21
v^{4s}_T	230–290	150–190	2000	17

[a] See Ref. 21.

-14-

up and the L distribution (and tail of Γ distribution) begin to flatten (see Fig. 2). Again, strong intervalley scattering drives the tail of the L distribution (and the part of the Γ distribution above the threshold for scattering into the X valleys) into equilibrium with the X distribution. This distribution is nearly a Maxwellian at the lattice temperature. This behavior is similar to what happens between the L and Γ valleys at low fields.

At much higher fields (above 50 kV/cm), the X distribution also heats up. This leads to the heating of which in turn heats up the tail of the Γ and the L distributions, and all three distributions begin to flatten (see Fig. 2). In this model, there are no other mechanisms for cooling the tails of the distributions. As previously mentioned, scattering into the X valleys prevents the population inversion in the Γ valley to become as pronounced as in a two-valley model. For the fields investigated no population inversion is observed in the L or Γ valleys due to the flux of electrons from the X valleys near threshold, although the trend for such a condition is evident.

2. Rate coefficients

Macroscopic (moment) descriptions of carrier dynamics in semiconductors require knowledge of the rate coefficients that appear in the corresponding equations. In a one-moment description (in terms of the continuity equations for carrier densities), the necessary rates are the averaged carrier gain or loss rates. At applied fields for which the population of the upper valleys becomes significant, a multivalley macroscopic description is desirable. In this case, carrier gain or loss in each valley is due (at low carrier densities and at fields for which impact ionization is negligible) to intervalley scattering.

With the code described in Sec. II, we have obtained the averaged (over the distribution) intervalley scattering rates for carrier gain or loss as a function of applied field. The rates are shown in Fig. 3. These rates are defined as follows:
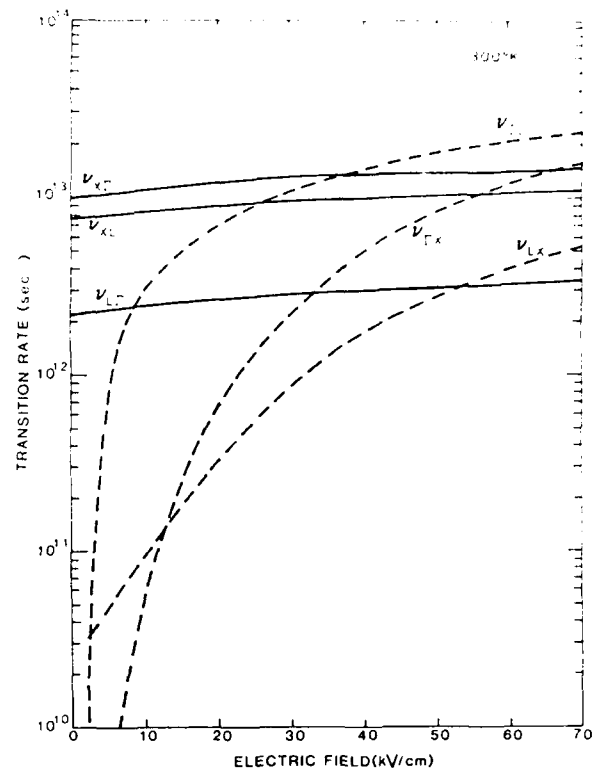

FIG. 3. Averaged transition rates as a function of applied electric field. Solid lines represent the transition rates from upper to lower valleys. Dashed lines represent the transition rates from lower to upper valleys.

$$N_i \nu_{ij} = \int S_{ij}(\mathbf{k}) f_i(\mathbf{k}) d\mathbf{k} ,$$

where i and j represent the Γ, L, or X valleys, S_{ij} is the microscopic intervalley scattering rate from the i valley to the j valley, f_i is the distribution in the i valley, and N_i is the population of the i valley. Their field dependence follows from the behavior of the distributions and the microscopic intervalley scattering rates. Since the microscopic scattering
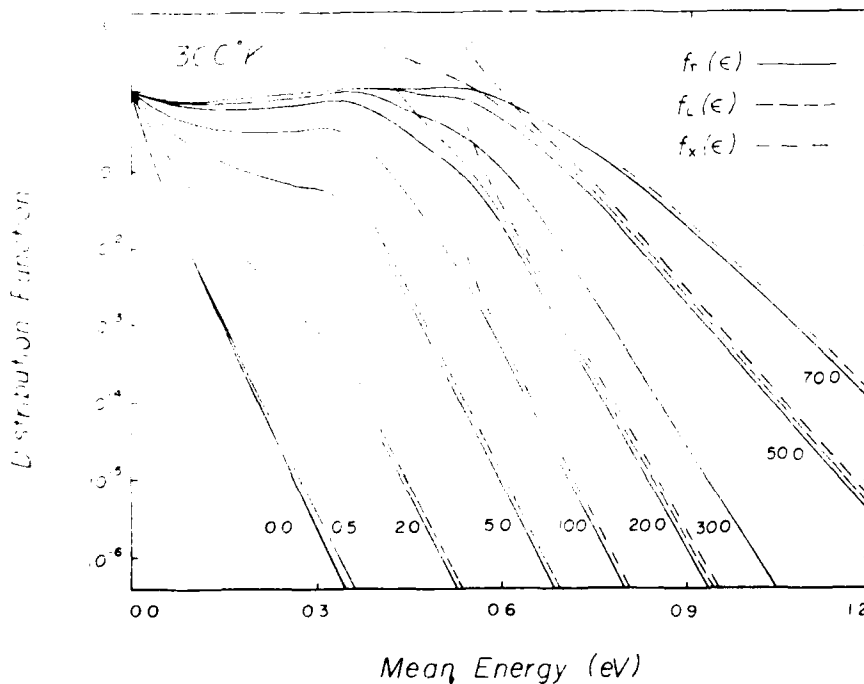

FIG. 2. Energy distributions of electrons in each valley of GaAs for different electric fields. The numbers correspond to the applied electric fields in kV/cm.

Mean Energy (eV)

-15-

rates from the upper to lower valleys have no strong energy dependence, and the distribution function in the upper valleys does not change significantly with field (see Fig. 2), the folding of the two functions lead to nearly constant average macroscopic rates. On the other hand, scattering from lower to upper valleys involves the tail of the corresponding distributions; since only electrons with energy above the threshold can participate). Since the tail of the distribution are very sensitive to the field, the folding of the two functions is strongly field dependent.

At low fields the average rates for scattering into the upper valleys are smaller than their respective inverse rates. As the field increases above 3.5 kV/cm (see Fig. 3), the average scattering rate into the L valleys, $v_{\Gamma L}$, becomes comparable to its inverse $v_{L\Gamma}$ (higher than 10% of $v_{L\Gamma}$), and the population of electrons in the L valleys increases drastically (see Fig. 4). Above 35 kV/cm, the average scattering rates into the X valleys, $v_{\Gamma X}$ and v_{LX}, become comparable to their respective inverses. $v_{X\Gamma}$ and v_{XL}, resulting in an increase in the population of the X valleys with a concomitant decrease in the population of the L valleys (see Fig. 4). As previously mentioned at these fields, the tail of the distributions heat up due to the heating up of the population (see Fig. 2). The scattering out of the X valleys into the L and Γ valleys is greater that out of the L valleys into the Γ valley. This has a considerable effect on the dynamics of the carriers at these fields in steady state and in transient situations. This is illustrated in the next section with regards to the steady-state transport parameters.

3. Average velocity and mean energy

The technique discussed in Sec. II has permitted the use of a large number of electrons in our simulations. As a consequence, we have been able to observe steady-state transport properties which are not clearly exhibited in simulations with large fluctuations (small number of particles). Here, we present the results we have obtained for the average velocity and the mean energy for electrons in each valley.

The average velocity in each valley is shown in Fig. 5(a) as a function of field. Also shown is the total average velocity (v) (averaged over all electrons irrespective of their valley) and representative experimental results.[20,25,26] The total average velocity has a maximum at a field equal to 3.8 kV/cm and rapidly decreases with increasing field until it becomes nearly constant for fields above 10 kV/cm [see Fig. 5(a)]. This behavior is well known and is the result of intervalley scattering (which is isotropic) and the fact that the electrons have a higher effective mass in the upper valleys.

At low fields (below 10 kV/cm), our calculations of average velocity are in good agreement with the results of Ruch and Kino.[25] However, the calculated peak velocity is slightly lower than the experimental value which occurs at 3.5 kV/cm. In the high field range (above 20 kV/cm), our calculations of average velocity fit the data of Riginos[26] quite well for values of fields up to 70 kV/cm. These values are 16% higher than those obtained by Houston and Evans.[30] These differences are reflected in the values of the material parameters used in the calculations (see Table I). The fraction of the electron population in the upper valleys as a function of field is shown in Fig. 5(b). This figure covers the range of fields near the maximum of the total average velocity and illustrates the decrease in $\langle v \rangle$ as the population in the upper valleys increases. The Γ valley average velocity $\langle v_\Gamma \rangle$ is observed to reach a maximum at a larger field, namely 5.5 kV/cm.[27] Between 5.5 and 10 kV/cm, $\langle v_\Gamma \rangle$ makes a "transition" to a lower value and remains nearly constant with field until at 35 kV/cm a second "transition" to a lower value is observed. These transitions have, in part, the same origin; namely, the fact that intervalley scattering is isotropic. For
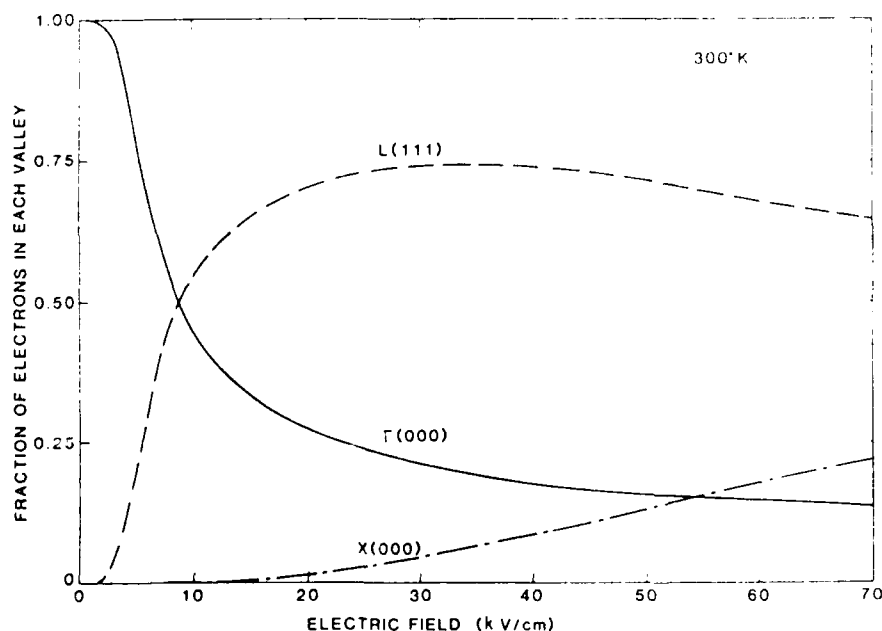

FIG. 4. Fraction of electrons in each valley as a function of applied electric field.

fields above the first critical field, scattering from L valleys to Γ valley randomizes the electron momentum in the Γ valley and thus decreases $\langle v_\Gamma \rangle$. At high fields above the second critical field, the population in the L valleys is observed to decrease with a concomitant increase in the population of the X valleys (see Fig. 4). Since the scattering from the X valleys into the Γ valley is always larger than scattering from the L valleys, there is an increase in the number of electrons with random momentum transferred into the Γ valley above 35 kV/cm. This effect lowers the average velocity. A slight decreases in the slopes of both $\langle v \rangle$ and $\langle v_\Gamma \rangle$ are also observed. From Fig. 5, the mobilities in the linear region are calculated to be 8800, 520, and 110 cm²/V s for the Γ, L, and X valleys, respectively.

The average electron energy in each valley relative to its lowest energy are illustrated in Fig. 6. For low fields, the electron energy in the Γ valley increases rapidly with field. In this range the dominant scattering process is invariant polar scattering. Above 10 kV/cm, where population inversion is observed in the Γ valley, the strong intervalley scattering process takes energetic electrons out of the Γ valley, thus reducing the rate of average energy increase. In the upper valleys, the average energy varies almost linearly with field. This is due to the high intervalley scattering rate in the upper valleys.

IV. CONCLUDING REMARKS

In this paper, a technique for implementing the Monte Carlo Method with self-scattering has been presented. This technique leads to large savings in computational time, and thus allows, for a given CPU time, an increase in the number of test particles used in the simulation. This reduces the statistical fluctuation in the calculated quantities. With a code that uses this technique, we have investigated the steady-state behavior of electrons in a three-valley model of GaAs and influenced by a dc electric field.
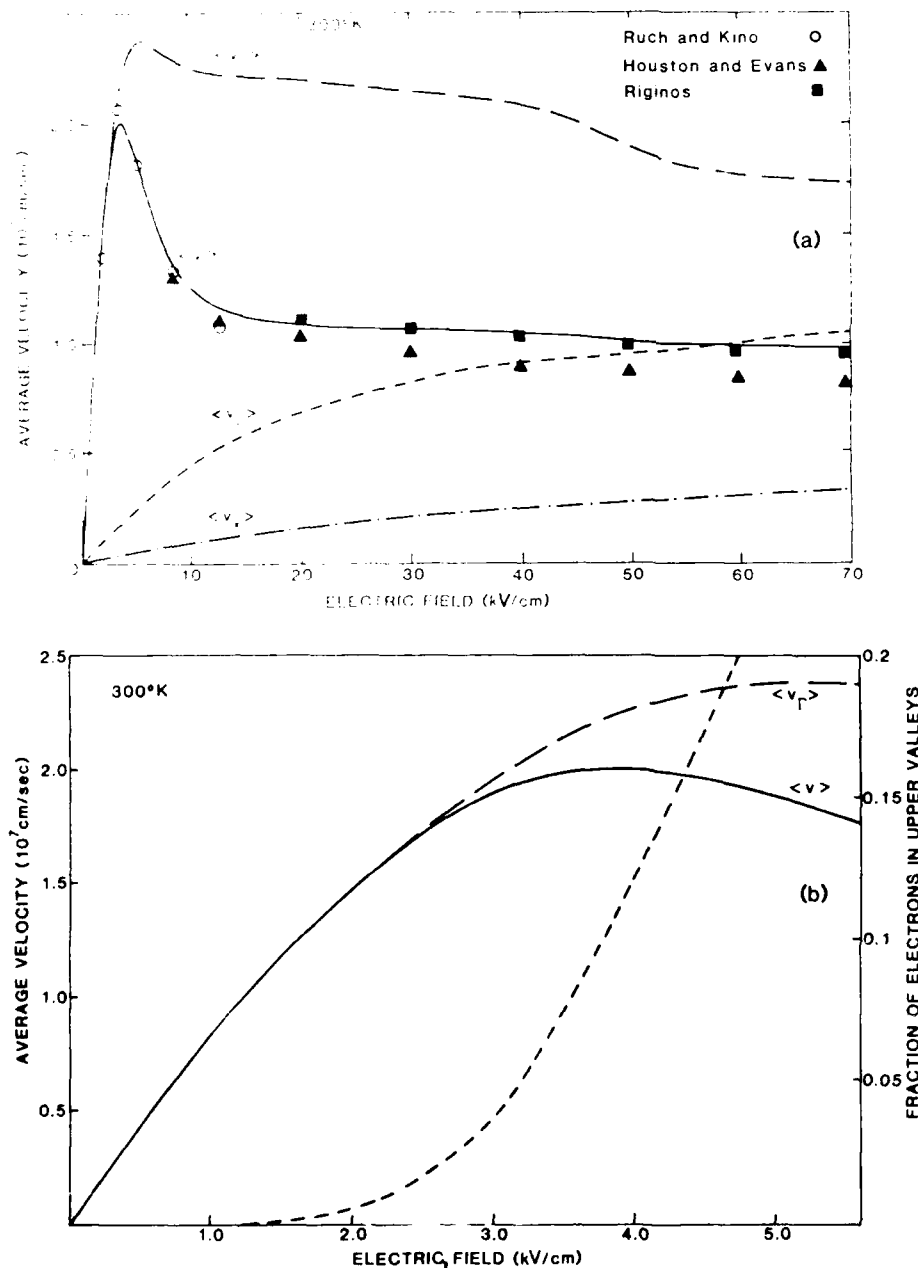

FIG. 5. (a) Total average velocity $\langle v \rangle$ and the average velocity in each valley as a function of applied electric field. Also included are the experimental results by Houston and Evans (see Ref. 20), Ruch and Kino (see Ref. 25), and Riginos (see Ref. 26). (b) Total average velocity $\langle v \rangle$, the average velocity in Γ valley $\langle v_\Gamma \rangle$, and the fraction of electrons in upper valleys (short dashed line) as a function of applied electric field for fields near and below the velocity maximum.
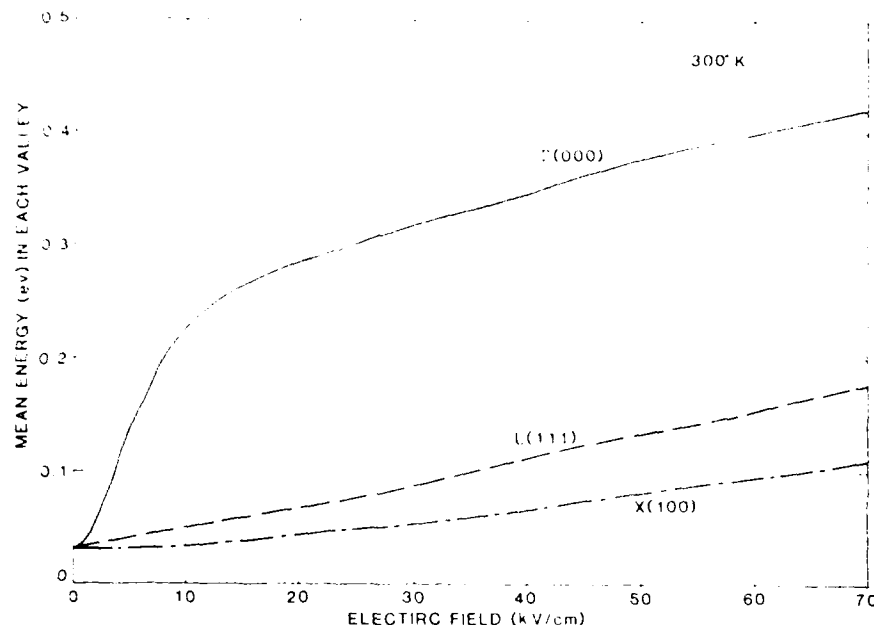
FIG. 6. Mean energy of electrons in each valley relative to its lowest energy as a function of applied electric field.

At low fields, the results obtained agree well with previous theoretical and experimental results. At high fields, we have observed a second transition region where the average velocity in the Γ valley rapidly changes with field. This change is due to the increase in the population of the X valleys and the large X-to-Γ scattering rate. This process also has an effect on the behavior of the distribution function, electron population in each valley, and the transport parameters for fields at and above the transition region. In particu-

lar, the population inversion observed in the Γ valley for fields above 10 kV/cm is not as pronounced (as it is in a two-valley model).

In fast transient situations, due to the differences in scattering rates, a three-valley model of GaAs is desirable for describing the dynamics of the carriers. The results presented in this paper can be used in the development of a three-valley hydrodynamic model.

[1]H. L. Grubin, D. K. Ferry, G. Iafrate, and J. R. Barker, *VLSI Electronics*, edited by N. G. Einspruch (Academic, New York, 1982), Vol. 3, p. 197.
[2]C. Jacoboni and L. Reggiani, Rev. Mod. Phys. **55**, 645 (1983).
[3]T. Kurosawa, J. Phys. Soc. Jpn. Suppl. **21**, 424 (1966).
[4]W. Fawcett, A. D. Boardman, and S. Swain, J. Phys. Chem. Solids **31**, 1963 (1970).
[5]P. J. Price, Semiconductors and Semimetals **14**, 249 (1979).
[6]E. E. Kunhardt and Y. Tzeng, J. Comput. Phys. **67**, 279 (1986).
[7]H. Budd, J. Phys. Soc. Jpn. Suppl. **21**, 420 (1966).
[8]P. J. Price, in *Proceedings of the 9th International Conference on the Physics of Semiconductors*, edited by S. M. Ryvkin (Nauka, Moscow, 1968), p. 753.
[9]H. D. Rees, J. Phys. Chem. Solids **30**, 643 (1969).
[10]H. Fröhlich, Proc. R. Soc. London Ser. A **188**, 521 (1947).
[11]W. Shockley, Bell Syst. Tech. J. **30**, 990 (1951).
[12]E. M. Conwell, *High Field Transport in Semiconductors*, Solid State Physics Suppl. 9 (Academic, New York, 1967).

[13]H. D. Rees, Phys. Lett. A **26**, 416 (1968).
[14]E. M. Conwell and M. O. Vassell, Phys. Rev. **166**, 797 (1968).
[15]C. Herring and E. Vogt, Phys. Rev. **101**, 944 (1956).
[16]W. Fawcett and E. G. S. Paige, J. Phys. C **4**, 1801 (1971).
[17]P. A. Lebwohl and P. J. Price, Solid State Commun. **9**, 1221 (1971).
[18]M. A. Littlejohn, J. R. Hauser, and T. H. Glisson, J. Appl. Phys. **48**, 4587 (1977).
[19]J. Pozela and A. Reklaitis, Solid State Commun. **27**, 1073 (1978).
[20]P. A. Houston and A. G. R. Evans, Solid State Electron. **21**, 197 (1977).
[21]The simulations were carried out in a Micro-Vax II.
[22]W. Fawcett and H. D. Rees, Phys. Lett. A **28**, 731 (1969).
[23]J. G. Ruch and W. Fawcett, J. Appl. Phys. **41**, 3843 (1970).
[24]D. Pines, *Elementary Excitations in Solids* (Benjamin, New York, 1963), Chap. 3.
[25]J. G. Ruch and G. S. Kino, Phys. Rev. **174**, 921 (1968).
[26]V. E. Riginos, J. Appl. Phys. **45**, 2918 (1974).
[27]T. J. Maloney and J. Frey, J. Appl. Phys. **48**, 781 (1977).
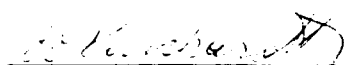
V. ABSTRACTS FOR PRESENTED PAPERS

Sorting Category
20c

Moment Descriptions of Electron Transport in Multi-
valley Semiconductors.* M. CHENG, E. E. KUNHARDT, Weber
Research Institute, Polytechnic U. -- A multi-valley moment
description of carrier transport in semiconductors is presented that
makes no apriori assumptions about the shape of the carrier
distribution in $\underline{k}$ space. It is based on the macro-kinetic model[1] for
electron transport. In this model, a macro-kinetic distribution
function is obtained in terms of carrier mean energy and
momentum. This distribution is then used to evaluate the
unknown rates and parameters in the multi-valley moment
equations. To illustrate the theory, the results obtained from
single-valley and multi-valley moment equations are compared to
those obtained from a Monte Carlo method using a multi-valley
model.

[1] E. E. Kunhardt, M. Cheng and C. Wu, J. Appl. Phys., 64, 1220
(1988).

Erich E. Kunhardt
Route 110
Farmingdale, NY 11735

Sorting Category
20c

Macro-Kinetic Models of Electron Transport in
Semiconductors.* E. E. KUNHARDT, M. CHENG, Weber
Research Institute, Polytechnic U. -- A nonequilibrium macro-
kinetic model that describes the behavior of carriers in a
semiconductor subjected to space-time varying fields has been
developed. The model is obtained by proper closure of the
moment equations through the introduction of a macroscopic
carrier distribution function, f_M. This distribution is shown to obey
a macro-kinetic equation[1] which, together with the finite set of
moment equations, constitutes the model. This set can be used to
describe the nonequilibrium behavior of carriers in the time scale
corresponding to the characteristic times of the moment equations.
Three levels of descriptions have been obtained by ordering the
moment equations according to the characteristic times. The first
three characteristic times are ordered as follows: $\tau > \tau_\varepsilon > \tau_m$,
where τ, τ_ε, and τ_m are carrier, energy and momentum relaxation
times, respectively. The first (S_1), second (S_2) and third (S_3)
levels of descriptions are valid for times in the order of τ, τ_ε, and
τ_m, respectively. Results obtained for carrier transport in GaAs
are presented.

[1] E. E. Kunhardt, M. Cheng and C. Wu, J. Appl. Phys., 64, 1220
(1988).

Erich E. Kunhardt
Route 110
Farmingdale, NY 11735